Renewable Energy Focus 49 (2024) 100573

Contents lists available at ScienceDirect

Renewable Energy Focus

journal homepage: www.journals.elsevier.com/renewable-energy-focus

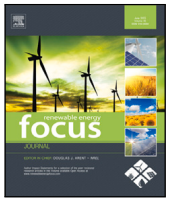

Research paper

Integration of optimal power flow with combined heat and power dispatch of renewable wind energy based power system using chaotic driving training based optimization

Chandan Paul [a,*], Tushnik Sarkar [a], Susanta Dutta [a], Provas Kumar Roy [b]

[a] Department of Electrical Engineering, Dr. B C Roy Engineering College, Durgapur, West Bengal, India
[b] Department of Electrical Engineering, Kalyani Government Engineering College, Kalyani, West Bengal, India

ARTICLE INFO

Keywords:
Chaotic driving training based optimization (CDTBO)
Combined heat and power economic dispatch (CHPED)
IEEE-30 bus
Optimal power flow (OPF)
Wind energy

ABSTRACT

Combined heat and power economic dispatch (CHPED) based optimal power flow (OPF) problem has been studied in this article using a new, practical approach based on chaotic driving training optimization (DTBO) (CDTBO). In the proposed technique (CDTBO), the chaotic based learning is integrated with DTBO to overcome the local optimal problem and inferior convergence speed of the existing algorithms. OPF is an important concern to retain the power system running effectively. In order to meet the demand for reasonably priced power generation with optimal power flow in transmission lines, the authors combined CHPED and OPF. Since fuel is changing daily in the current environment, using renewable energy sources to generate electricity economically is crucial. The renewable energy source like wind energy is integrated with thermal units for economic power generation with reducing the thermal fuel consumption of CHPED-based OPF system. The proposed technique implemented on CHPED based IEEE-30 bus system for renewable and without renewable energy sources with considering different cases. The suggested problem considering with valve point loading of thermal units, transmission losses and uncertainties of wind speed to address the non-linearity of the renewable-based CHPED-OPF system. Cost minimization, voltage deviation control, transmission losses minimization and stability index are the single objectives of the prospective system. Furthermore tested on multi-objective functions for simultaneously minimization of cost with emission and simultaneously minimization of active power loss with voltage profile. It is observed that the proposed CDTBO technique helps to reduce the cost by 2% and 12.8% for renewable based system as compared to non-renewable system for multi-objective function. The robustness of the proposed solution has been verified by implementing the statistical analysis on two systems with least variation of mean and optimal values of cost with the tolerance of less than 0.0035%. A comparison has been made with recent well known optimization techniques to address the superiority of the suggested CDTBO algorithm.

1. Introduction

Heat is released into the environment at all thermal power plants during the generation of electricity, either by cooling towers, flue gas, or some other means. The energy efficiency of power generation units drops to a very low level (between 50% and 60%) due to the byproducts produced during heating, such as NOX, SOX, SO2, and CO2. As a result, the atmosphere becomes contaminated. Problems with combined heat and power economic dispatch (CHPED) are important in power system research. The number of pollutants discharged into the atmosphere and the cost of production are reduced by using the waste heat from the steam. Chillers are used by the heat recovery steam generator in CHPED to recover heat lost during cooling and steam production. A co-generation system that produces both heat and electricity at the same time is the CHPED. CHPED raises the efficiency of thermal generating stations to above 75% even though it requires more capital.

Economic power generation was the primary emphasis of the CHPED, not transmission line power flow. Optimal power flow (OPF) in power systems is a well-studied optimization problem. This problem was first raised in 1962 by Carpentier [1]. The objective of OPF is to identify a steady state operating point that, at the same time lowering the cost of generating electricity, meets demand and operating constraints. Therefore, in order to meet the demand for reasonably priced power generation with optimal power flow in transmission

* Corresponding author.
E-mail address: chandan815@rediffmail.com (C. Paul).

https://doi.org/10.1016/j.ref.2024.100573
Received 14 September 2023; Received in revised form 1 March 2024; Accepted 19 April 2024
Available online 27 April 2024

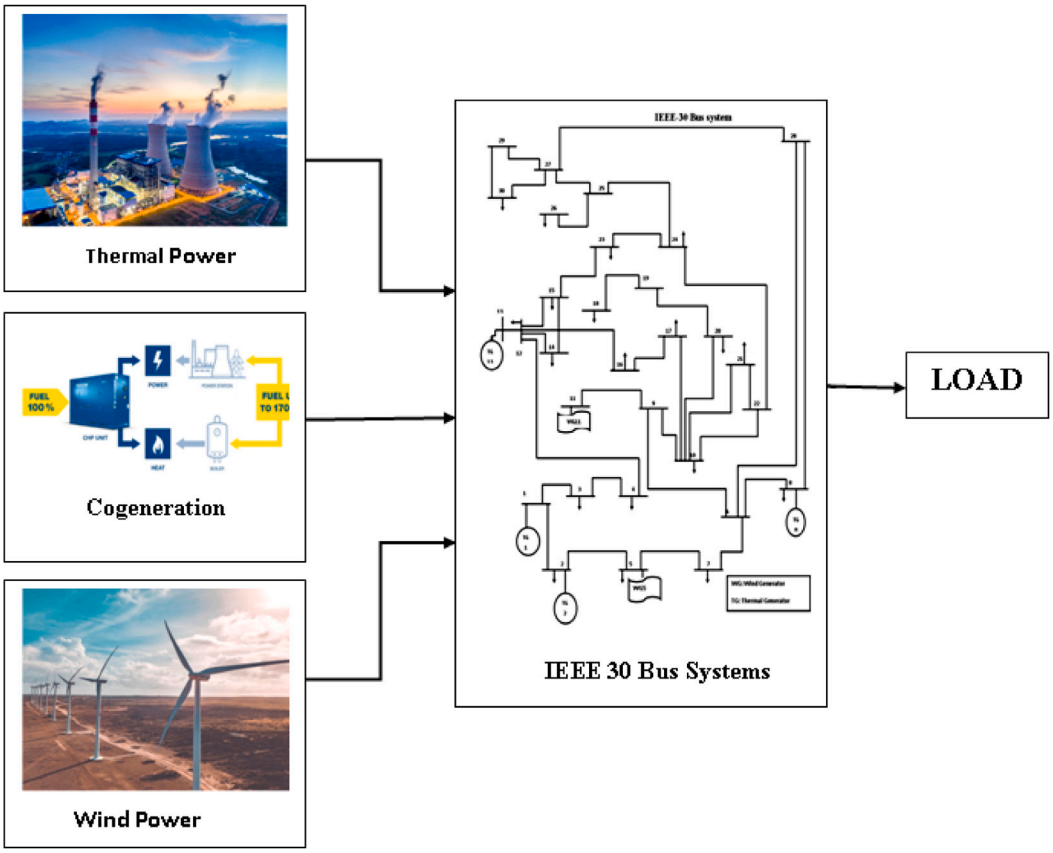

Fig. 1. Schematic model of CHPED based OPF with renewable energy.

lines, CHPED and OPF must be connected. Over the past few decades, researchers investigating electrical power systems have focused on developing different optimization methodologies to address the optimal power flow (OPF) problem. Taking into consideration all of the many power system restrictions, OPF looks for a practical solution that takes into account a number of important factors, such as economics, the environment, dependability, security, and power quality.

In the early phases of OPF issues, researchers were hired with the sole goal of obtaining the lowest fuel cost—by using thermal generators. However, a growing number of renewable energy sources must be integrated into the current power networks over time because of a number of causes, including the need for a carbon tax, the depletion of fossil resources, environmental regulations, and growing power usage. It goes without saying that attempting to employ alternative energy sources makes the network far more challenging. The extremely non-convex and nonlinear OPF problem has been tackled in the literature through the application of several evolutionary approaches. Limitations on network capability, generator capacity, power balance, and fuel emissions can be met while minimizing the cost of generation, active power loss, fuel emission, and voltage deviation by modifying the generators' schedules, terminal voltages, tap settings, and VAR compensation.

Many studies on single- and multi-objective functions utilizing various optimization strategies while satisfying all constraints have been presented by various researchers during the past two decades. The Lagrangian relaxation (LR) [2], the statistical process control method [1], linear programming [3], nonlinear programming [4], quadratic programming [5], and the interior point [6] were among the various classical techniques that had been tested on CHPED and OPF. Non-differentiable and nonlinear functions cannot be handled by classical methodologies because they are dependent on differential calculus and numerical techniques.

Many authors used various evolutionary-based optimization strategies to achieve the global optimum solution in order to solve the local optimum problem of nonlinear based challenges. In order to find the best solution for cost reduction, Beigvand et al. [7] used the gravitational search algorithm (GSA) on the CHPED while taking valve point loads and transmission losses into account. To assess its resilience on the CHPED system, Meng et al. [8] presented crisscross optimization with vertical crossover probability. Exchange market algorithm (EMA) was used by Ghorbani [9] to test its effectiveness in solving the nonlinear based CHPED problem. Smart searching is a foundational component of EMA, which aids in optimizing the limitations. For the purpose of obtaining the best solution for several test studies, Davoodi et al. [10] tested the modified group search optimizer (MGSO) on the CHPED issue with the scrounger and ranger operators. Paul et al. [11] applied whale optimization technique (WOA) on CHPED problem considering with non-linearity like valve point loading (VL) and prohibited operating zone (POZ) of thermal units for optimal solution. In order to generate power economically, Ramachandran [12] developed a hybrid model and applied it to the CHPED problem to investigate the effectiveness and robustness of the proposed technique. Betar et al. [13] suggested hybrid Harris Hawks with significant performance for the economic load dispatch (ELD) problem. Gholamghasemi et al. [14] recommended phasor particle swarm optimization (PPSO) for economic power generation on ELD based system with considering different constraints like transmission losses, ramp rate function and prohibited operating zone to judge the superiority of the proposed algorithm on real base system. Real coded chemical reaction algorithm (RCCRA) utilized by Bhattacharya et al. [15] on economic emission load dispatch (EELD) problem to solve multi-objective functions with minimizing both cost and emission.

Yuan et al. [16] utilized artificial bee colony algorithm (ABC) integrated with quantum inspired chaotic based learning (QC) to increase the searching ability for global solution of optimal power flow

Table 1
A collection of various chaotic maps.

Sl. No.	Name	Chaotic map
N1	Circle	$r_{k+1} = r_{k+b} - (a/2\pi)sin(2\pi k)\, mod\ (2)$
N2	Cubic	$r_{j+1} = ar_j\left(1 - r_j^2\right)$
N3	Chebyshev map	$r_{j+1} = \cos\left(k\cos^{-1}\left(r_k\right)\right)$
N4	Logistic map	$r_{k+1} = ar_k\left(1 - r_k\right)$
N5	Gussian map	$r_{k+1} = r_{k+1}\begin{cases}0, & r_k = 0,\\ \frac{1}{r_k} \bmod (1) = \frac{1}{r_k} - \left[\frac{1}{r_k}\right]\end{cases}$
N6	Liebovitch map	$r_{k+1} = ar_k\left(1 - r_k\right)$
N7	Iterative map	$\mathrm{r_{k+1}} = \mathrm{Sin}\left(\frac{\mathrm{a}\pi}{\mathrm{rk}}\right), \alpha \in (\mathrm{U},\ 1)$
N8	Sine	$X_{i+1} = a/4\left(sin\prod x\right)$
N9	Sinusoidal	$X_{i+1} = a\left(X_i\right)2\left(sin\prod x_i\right)$
N10	Tent	$X_{i+1} = \begin{cases}\frac{X_i}{0.7};\ \mathrm{X}_i < 0.7\\ \frac{10}{3}(1 - X_i)\ ;\mathrm{X}_i \geq 0.7\end{cases}$

Table 2
Comparison of statistical results of CDTBO.

Optimization techniques	Cost ($/h)			Computational time (s)
	Minimum	Mean	Maximum	
CDTBO1	14 558.1285	14 581.4765	14 595.3976	4.76
CDTBO2	14 562.1257	14 570.2546	14 578.1298	4.25
CDTBO3	14 555.3256	14 564.7863	14 569.0186	3.96
CDTBO4	14 560.7684	14 566.1243	14 577.6986	3.82
CDTBO5	14 553.9658	14 561.1298	14 571.6658	3.94
CDTBO6	14 553.6723	14 560.8954	14 570.5846	3.68
CDTBO7	14 552.9845	14 558.9931	14 565.7462	3.45
CDTBO8	14 563.5645	14 572.1278	14 590.3687	4.18
CDTBO9	14 552.5479	14 558.6823	14 564.2323	3.32
CDTBO10	14 554.8636	14 566.7227	14 578.6622	3.38
DTBO	14 554.4097	14 560.1265	14 575.7283	3.68

(OPF) problem. In order to determine the best location for UPFC for producing electricity economically while maintaining the restrictions of the power system of the OPF issue, In order to determine the best location for UPFC for producing electricity economically while maintaining the restrictions of the power system of the OPF issue, Dutta et al. [17] used the chemical reaction optimization approach (CRO). In order to assess the superiority of the KHA strategy on the OPF problem, Roy and Paul [18] demonstrated how to use the krill heard algorithm (KHA). Several IEEE bus systems were used to evaluate the KHA technique, and comparisons with other optimization techniques were made. Lee et al. [19] had devised the OPF formulation for a bipolar DC microgrid. This system optimizes the cost, voltage deviation, and transmission losses by combining a bipolar DC microgrid with distributed generators (DGs). On several buses of an integrated feeder-based distribution generator for OPF with diverse objective functions, Shahhen et al. [20] performed heap-based optimization. The improved mayfly algorithm (IMA) was introduced by Bhaskar et al. [21] in order to determine the best outcome for cost minimization, voltage deviation, and transmission losses on the IEEE 30 bus system, hence assessing the efficacy of the employed technique. Fergany and Hasanien conducted testing of the tree seed method on multiple buses with various multi-objective functions with optimal flow across transmission lines [22]. To find out if the applied method is better than the others, Xiao et al. [23] proposed an optimization strategy based on meta-models. Different search algorithms (DSAs) were applied by Abaci and Yamacli [24] on IEEE-9, 30, and 57 bus systems for OPF, with cost, variable load, and shunt capacitance parameters controlled. To effectively solve the OPF problem, Bouchekara et al. [25] used improved colliding bodies optimization (ICBO) on 16 different scenarios. Oppositional based learning was merged with the gravitational search algorithm (GSA) (OGSA) by Bhowmik and Chakraborty [26] to solve the local optimal issue and achieve the multi-objective solution for the IEEE-30 bus system. The krill heard algorithm (KHA), which helps to simultaneously balance cost and dynamic stability, was introduced by Mukherjee et al. [27] to tackle the OPF problem while taking transient stability into consideration. In order to get a global optimal solution for the OPF problem of various single and multi-objective functions, Mandal et al. [28] suggested a TLBO optimization technique combined with quasi oppositional based learning.

Fuel is a resource that is always evolving in the current environment, thus using renewable energy sources to provide economic power is crucial. Many researchers combined conventional power generating units with renewable energy sources to lower the amount of fuel needed to generate economically viable power. For an efficient and emission-free operation, Hazra and Roy [29] suggested moth flame optimization (MFO) on the HTS problem in conjunction with renewable energy. WOA combined with chaotic based learning (CWOA) was evaluated by Paul et al. [30] on two test systems of the CHPED issue while taking wind energy sources into account for the production of economically viable power. In order to minimize the use of thermal power units and limit the usage of renewable energy sources that are also integrated with the CHPED problem, Paul et al. [31] proposed quasi-oppositional based learning WOA (QOWOA) on CHPED system in addition to taking into account the VL and POZ. To further deal with greater non-linearity caused by the rising number of non-conventional energy sources with CHPED system, Paul et al. [32] integrate chaotic based learning with QOWOA (CQOWOA) to get the best results. In order to achieve realistic optimization control, the gradient tracking optimization technique was proposed by Zhang et al. [33] to assess the short-term OPF problem on IEEE 39-bus and 118-bus systems while taking wind power generation into consideration. To achieve optimal outcomes in terms of economic operation and mitigating the greenhouse effect, Evangeline and Rathika [34] introduced the horse herd algorithm (HHA) for the multi-objective OPF problem. focused on controlling transmission losses and voltage deviation in order to achieve the optimal power flow in the transmission line. The system uses wind power generation, which lowers pollution and fuel consumption. Li et al. [35] integrated non-conventional energy sources with the proposed solution for the IEEE 30 and 57-bus OPF challenge. In order to lower the uncertainty of wind speed and sun intensity, Weibull and lognormal PDF are utilized. In order to address the impact of renewable energy sources on the OPF problem while accounting for transitory stability limits, Chen *etal*. [36] proposed semi-define programming (SDP) for the 39-bus system. To find the optimal solution for both single- and multi-objective cost and emission functions, Sulaiman et al. [37] introduced teaching learning based optimization (TLBO) on the wind-solar based OPF problem. Using an adaptive differential evolution methodology on a renewable-based OPF problem, Biswas et al. [38] assessed the efficacy of the proposed method in comparison to cost-effective power generation. For the purpose of validating the proposed technique over cost reduction, Elephant clan optimization (ECO) for renewable-based dynamic OPF problem on several IEEE buses and 15 bus micro-grid was proposed by Basu [39].

Ozkaya et al. [40] proposed artificial rabbit optimization (ARO) to analyze the CHPED problem where adaptive fitness distance balance has been integrated with ARO (AFDB-ARO) to improve the exploration capability of the proposed technique. In the proposed system, valve point loading (VPL), prohibited operating zone (POZ) and transmission losses have been considered to test the performances of AFDB-ARO on real based problem. Moreover, Ozkaya et al. in their recent endeavor [41] utilized symbiotic organism search algorithm based on dynamic switched crowding for optimal solution of the economic emission dispatch problem with CHPED.

The literature research demonstrates that the following features of the current optimization schemes: (i) Different non-linear based problem effectively solved, (ii) the above population based optimization techniques are derivative free, (iii) for the majority of the present techniques, robustness can be proven. Despite the fact that the power system's performance has improved thanks to the existing technologies, these systems have some drawbacks (i) the rate of convergence for the

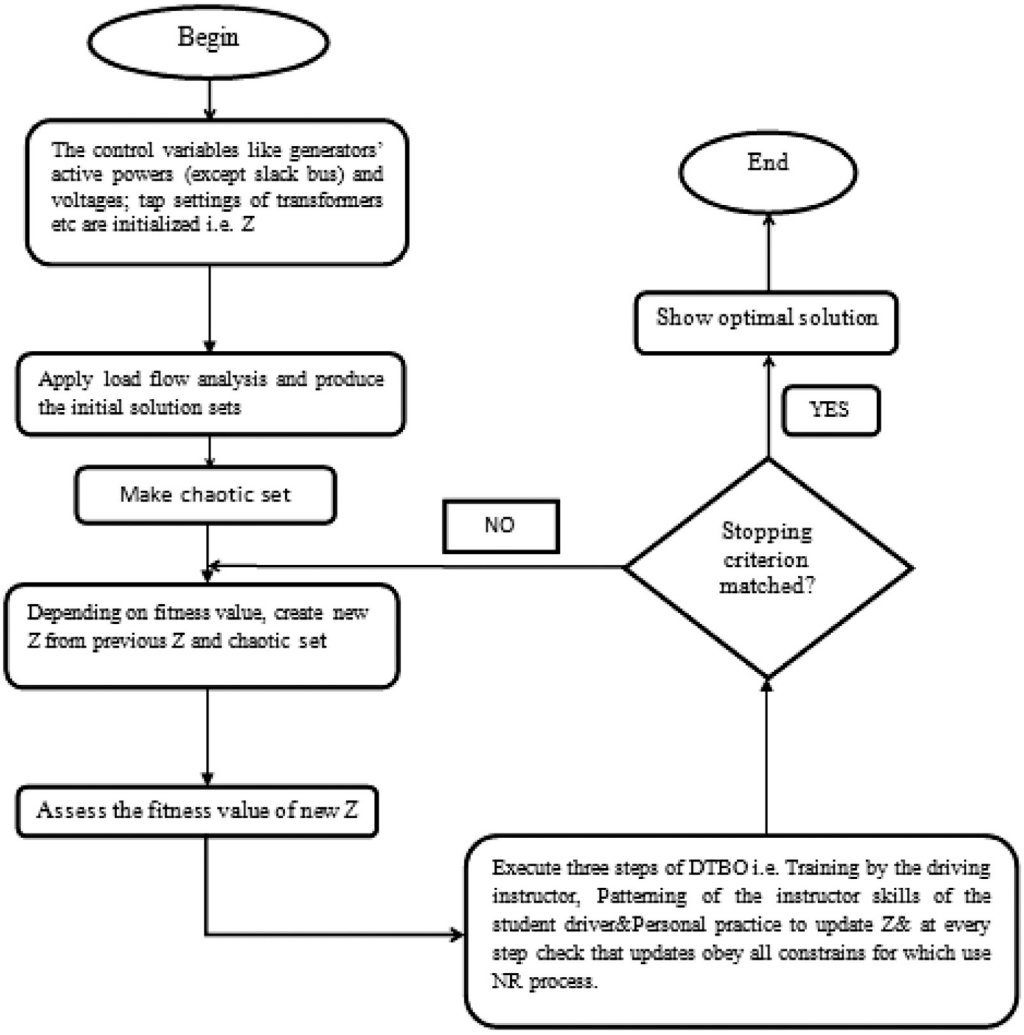

Fig. 2. Flowchart of CDTBO optimization technique.

Table 3
Various case-studies investigated in this article.

case	Single objective	Multi objective	Considered objectives	Constraints	Test system
1	✓		Total Cost minimization with valve point effects	Equality and non-equality	
2	✓		Emission and carbon tax minimization	Equality and non-equality	
3		✓	Simultaneous minimization of Cost with Emission and carbon tax	Equality and non-equality	
4	✓		Active power loss minimization	Equality and non-equality	IEEE 30 Bus
5	✓		Voltage profile minimization	Equality and non-equality	
6	✓		Voltage stability minimization	Equality and non-equality	
7		✓	Simultaneous minimization of Active power loss and Voltage profile	Equality and non-equality	
8	✓		Total Cost minimization with valve point effects for thermal, and wind energy	Equality and non-equality	
9	✓		Emission and carbon tax minimization	Equality and non-equality	
10		✓	Simultaneous minimization of Cost with Emission and carbon tax	Equality and non-equality	
11	✓		Active power loss minimization	Equality and non-equality	Wind based IEEE 30 Bus
12	✓		Voltage profile minimization	Equality and non-equality	
13	✓		Voltage stability minimization	Equality and non-equality	
14		✓	Simultaneous minimization of Active power loss and Voltage profile	Equality and non-equality	

aforementioned methods is low. Most of the aforementioned algorithms suffer from early convergence, which lowers their performance and limits their ability to explore, yielding solutions that are not optimal. (ii) there is chance to trapped into the local optima, (iii) low exploration and exploitation capability In order to get beyond the aforementioned shortcomings, the contemporary authors were inspired to use a novel optimization technique.

The main contributions of the paper are as follows:

- An integrated CHPED with OPF scheduling model Fig. 1 considering renewable energy source is proposed.
- Different single objective functions has been discussed like cost minimization, emission minimization, transmission loss minimization, voltage profile minimization, voltage stability control and various multi-objective functions like cost-emission, active power loss with voltage profile.

- The suggested optimization technique's robustness has been assessed by statistical analysis.

The rest of the paper is structured as follows: The details of wind power generating are included in Section 2. Section 3 shows how the suggested system formulates the problem. In Section 4, the various stages of the suggested optimization technique with flowchart have been covered. The different test systems with simulation results and statistical analysis has been illustrated in the Section 5. Section 6 of the proposed system reports its conclusion.

2. Details of wind power

Owing to its dependence on wind speed, which leads to zero emissions and reduced production costs, connecting wind power to other power sources is ideal in order to ensure a reliable supply of electricity, as wind power cannot meet all of the demand for it. Uncertainty in wind power affects the dispatch of power to the grid; this is discussed in more detail below.

2.1. Wind power uncertainty functions

Dispatchable energy sources of electricity are those that have the capacity to produce power as needed. However, the uncertainty of wind sources brought on by wind speed makes it difficult to integrate the wind units with the grid. The Weibull PDF is usually selected to depict wind speed, as (1) demonstrates.

$$F_{rand}(V_{wind}) = \frac{k}{d}\left(\frac{V_{wind}}{d}\right)^{k-1} \times e^{-\left(\frac{V_{wind}}{d}\right)^{k}} \tag{1}$$

where initial velocity of wind defined by V_{wind}; random value signifies with *ran*; $k > 0$ denotes the shape factor whereas $d > 0$ signifies scale factor. A representation of the cumulative density function (CDF) is shown in Eq. (2).

$$f_{rand}(V_{wind}) = 1 - e^{-\left(\frac{V_{wind}}{d}\right)^{k}} \tag{2}$$

Several researchers have assessed a linear model to estimate wind power (see (3)) by utilizing wind velocity.

$$P_{wind} = \begin{cases} 0 & V_{wind} < V_{in} \text{ or } V_{wind} > V_{out} \\ \frac{P_{wrated}(V_{wind} - V_{in})}{V_{rated} - V_{in}} & V_{in} \le V_{wind} < V_{rated} \\ P_{wrated} & V_{rated} \le V_{wind} < V_{out} \end{cases} \tag{3}$$

where P_{wind} and P_{wrated} are signify the wind output power and rated power; rated wind velocity denotes with V_{rated}; cut-in and cut-out velocity of wind represent with V_{in} and V_{out}; representation of PDF of P_{wind} illustrated in (4).

$$F_{P_{wind}}(P_{wind}) = \frac{ku}{dP_{wrated}}\left(\frac{V_{in} + u\frac{P_{wind}}{P_{wrated}}}{d}\right)^{k-1} \times e^{-\left(\frac{V_{in}+u\frac{P_{wind}}{P_{wrated}}}{d}\right)^{k}}$$
$$where \quad u = V_{rated} - V_{in} \tag{4}$$

The two discrete probabilities when P_{wind} equals 0 or P_{wrated}, the continuous probability is represented as follows:

$$\begin{cases} S_{rated}(P_{wind} = 0) = S_{rated}(V < V_{in}) + S_{rated}(V > V_{out}) \\ \quad = 1 - e^{-\left(\frac{V_{in}}{d}\right)^{k}} + e^{-\left(\frac{V_{out}}{d}\right)^{k}} \end{cases} \tag{5}$$

$$\begin{cases} S_{rated}(P_{wind} = P_{wrated}) = S_{rated}(V_{rated} \le V < V_{out}) \\ \quad = e^{-\left(\frac{V_{rated}}{d}\right)^{k}} - e^{-\left(\frac{V_{out}}{d}\right)^{k}} \end{cases} \tag{6}$$

CDF of P_{wind} is obtained by integrating Eqs. (5) and (6), which is illustrated in (7).

$$f_{P_{wind}}(P_{wind}) = \begin{cases} 0 & Pwind < 0 \\ \frac{ku}{dP_{wrated}}\left(\frac{V_{in}+u\frac{P_{wind}}{P_{wrated}}}{d}\right)^{k-1} & \\ \quad \times e^{-\left(\frac{V_{in}+u\frac{P_{wind}}{P_{wrated}}}{d}\right)^{k}} & 0 \le P_{wind} < P_{wrated} \\ 1 & P_{wind} \ge P_{wrated} \end{cases} \tag{7}$$

2.2. Determination of wind cost

When to schedule wind power generating units into the system during periods of peak load will depend on how unpredictable the wind is. The erratic wind speed along the coast creates uncertainty in the production of power. Weibull's PDF will be used to examine the anticipated uncertainty costs associated with wind energy. Overestimation and underestimation serve as definitions for this function (8).

$$TotalCost_{wind} = \sum_{m=1}^{N_{wind}} Cost_{windm}(P_{windm}) = \sum_{m=1}^{N_{wind}} \left(Cost^{O}_{windm} + Cost^{U}_{windm}\right) \tag{8}$$

where $TotalCost_{wind}$ represents the total wind cost and N_{wind} denotes the total number of wind units.

2.2.1. Overestimation cost of wind

The cost of overestimating is explained when the generated power is less than what was planned. This means the load need will not be satisfied by the wind-generated power. Spinning reserve will provide the additional power required to meet load demand. From (9), one may compute the cost of overestimation.

$$\begin{cases} Cost^{O}_{windm} = Pf^{O}_{windm} \times P_{windm}\left[1 - e^{-\left(\frac{V_{in}}{s}\right)^{j}} + e^{-\left(\frac{V_{out}}{s}\right)^{j}}\right] \\ \quad + \left(\frac{P_{wratedm}V_{in}}{V_{rated} - V_{in}} + P_{windm}\right)\left[e^{-\left(\frac{V_{in}}{c}\right)^{j}} - e^{-\left(\frac{V_{in}+P_{windm}\frac{V_{rated}-V_{in}}{P_{wrated}}}{s}\right)^{j}}\right] \\ \quad + \left(\frac{P_{wrated}s}{V_{rated} - V_{in}}\right)\left[\zeta\left\{1 + \frac{1}{j}, \left(\frac{V_{in}+P_{windm}\frac{V_{rated}-V_{in}}{P_{wrated}}}{s}\right)^{j}\right\}\right. \\ \quad \left. - \zeta\left\{1 + \frac{1}{j}, \left(\frac{V_{in}}{s}\right)^{j}\right\}\right] \end{cases} \tag{9}$$

2.2.2. Underestimation cost of windcalculation

Expenses associated with underestimating occur when actual wind energy exceeds predictions. Any extra electrical energy produced by wind turbines will be stored in batteries since otherwise produced electricity will be lost. The underestimating cost can be computed using

Table 4
An outline of the IEEE 30 bus for the CHPED system based on OPF.

Items	Quantity	Details
Buses	30	[ref]
Branches	41	[ref]
Thermal generators	6	2 power only units (buses 1, 2), 4 CHP units (buses 5, 8, 11 and 13) and 1 heats only unit
Tap changing transformer	4	Branches:(6–9), (6–10), (4–12) and (27–28)
Control variables	22	Scheduled real power for 5Nos. Generators; bus voltages of all generator buses (6Nos.) transformer tap setting (4 nos), compensation devices (2 Nos.), 5 heats unit.
Load demand, Heat demand		283.4 MW, 126.2 MVAr, 175 MWth
Range of load bus voltage	24	[0.95–1.05] p.u.
Compensation devices	2	Buses: 10 and 24

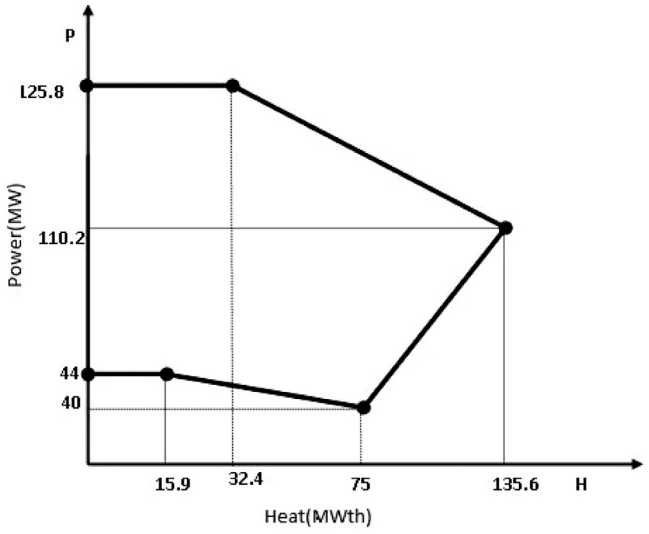

Fig. 3. Feasible region of CHP units (6th of 7-unit system).

the following formula (10):

$$\begin{cases} Cost^{U}_{windm} = Pf^{U}_{windm} \times \left(P_{wrated} - P_{windm}\right)\left[e^{-\left(\frac{V_{rated}}{s}\right)^{j}} - e^{-\left(\frac{V_{out}}{s}\right)^{j}}\right] \\ + \left(\frac{P_{wrated}V_{in}}{V_{rated}-V_{in}} + P_{windm}\right)\left[e^{-\left(\frac{v_{rated}}{s}\right)^{j}} - e^{-\left(\frac{V_{in}+P_{windm}\frac{v_{rated}-v_{in}}{P_{wrated}}}{s}\right)^{j}}\right] \\ + \frac{P_{wrated}s}{V_{rated}-V_{in}}\left[\zeta\left\{1+\frac{1}{j},\left(\frac{V_{in}+P_{windm}\frac{V_{rated}-V_{in}}{P_{wrated}}}{s}\right)^{j}\right\}\right. \\ \left. - \zeta\left\{1+\frac{1}{j},\left(\frac{V_{rated}}{s}\right)^{j}\right\}\right] \end{cases} \tag{10}$$

In the above equations overestimation and underestimation cost of mth wind unit signified with $Cost^{O}_{windm}$ and $Cost^{U}_{windm}$; rated output power and rated velocity denoted by P_{wrated} and V_{rated}; V_{in} and V_{out} are cut-in and cut-out velocity of wind; Pf^{U}_{windm} is underestimation and Pf^{O}_{windm} is overestimation cost co-efficient respectively.

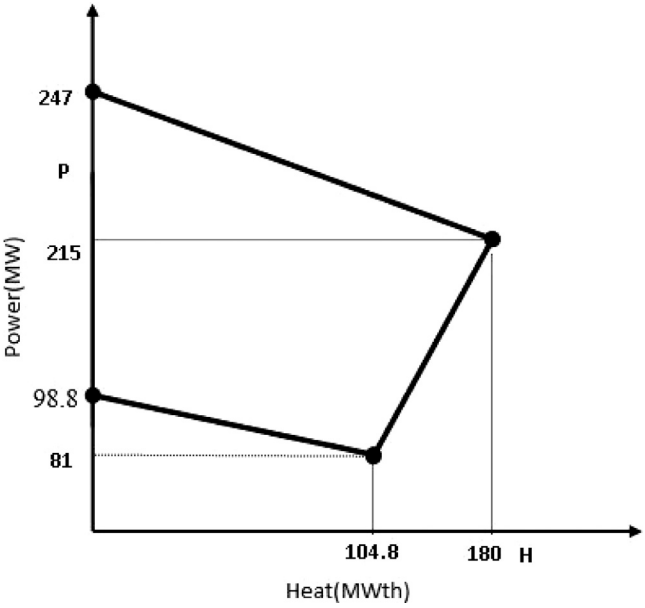

Fig. 4. Feasible region of CHP units (5th of 7-unit system).

3. Problem formulation

The CHPED-based OPF problem formulation in the IEEE-30 bus system is a crucial optimization strategy for monitoring the functioning of the power system. Less thermal unit usage for optimal power generation while meeting all generation and load balanced equation requirements is the problem formulation for CHPED scheduling. For cost-effective power generation with lower emissions, the CHPED-based OPF system's load-balanced problem formulation incorporates renewable energy sources as well. The followings illustrate the analytic version of the cost equation, the power balancing equation with and without renewable energy sources, and the equality and inequality restrictions.

3.1. Objective function

3.1.1. Case 1: CHPED based OPF system

The suggested CHPED-based OPF system's primary goal is shown by (11):

$$Minimum\ Cost = \sum_{i=1}^{N_{pou}} Cost_{poui}\left(P_{poui}\right) + \sum_{i=1}^{N_{chp}} Cost_{chpi}\left(P_{chpi}, H_{chpi}\right) + \sum_{i=1}^{N_{hou}} Cost_{houi}\left(H_{houi}\right) \tag{11}$$

where fuel cost of the power generator is manifested by $Cost_{poui}\left(P_{poui}\right)$; co-generation and heat unit generation costs showed up as $Cost_{ci}\left(P_{chpi},\ H_{chpi}\right)$ and $Cost_{houi}\left(H_{houi}\right)$; P_{poui} and H_{houi} signified the power and heat of ith unit; number of power, co-generation and heat only units manifested by N_{pou}, N_{chp}, N_{hou}.

The following formula represents the thermal cost function and expresses it as a quadratic cost function.

$$Cost_{poui}\left(P_{poui}\right) = \alpha_{poui}\left(P_{poui}\right)^{2} + \beta_{poui}P_{poui} + \gamma_{poui} \tag{12}$$

where α_{poui}, β_{poui} and γ_{poui} express the cost coefficients of the ith thermal unit.

The cost function equation analyzed and researched in (12) has been modified by accounting for the valve point loading in (13).

$$C_{poui}\left(P_{poui}\right) = \alpha_{poui}\left(P_{poui}\right)^{2} + \beta_{poui}P_{poui} + \gamma_{poui}$$

Table 5
Simulation results and control parameters of different cases for CHPED based OPF using DTBO.

Control parameters	Min.	Max.	Case 1	Case 2	Case 3	Case 4	Case 5	Case 6	Case 7
PTG1 (MW)	50	200	191.57	65.22	184.21	53.08	183.25	84.09	66.79
PTG2 (MW)	20	80	51.85	68.89	53.55	79.23	24.38	78.38	79.32
PTG5 (MW)	15	50	15.04	49.28	15.09	49.6	29.09	49.38	49.43
PTG8 (MW)	10	35	11.64	34.72	14.13	34.97	19.14	34.83	34.45
PTG11 (MW)	10	30	11.48	29.95	14.21	29.93	26.32	28.68	25.6
PTG13 (MW)	12	40	12	38.71	12.79	39.86	12.28	12.54	32.41
V1 (p.u.)	0.95	1.1	1.0987	1.0656	1.056	1.0392	0.998	1.0998	0.9971
V2 (p.u.)	0.95	1.1	1.0854	1.0569	1.0446	1.0379	0.9791	1.0903	1.0035
V5 (p.u.)	0.95	1.1	1.0574	1.0326	1.0111	1.0181	1.0145	1.0948	1.0134
V8 (p.u.)	0.95	1.1	1.064	1.0431	1.0212	1.0247	1.0131	1.0995	1.021
V11 (p.u.)	0.95	1.1	1.0999	1.0898	1.0583	1.0982	1.0922	1.0986	1.0348
V13 (p.u.)	0.95	1.1	1.0998	1.0984	1.0913	1.0996	1.0731	1.0964	1.0313
T11 (p.u.)	0.9	1.1	1.0277	0.9853	0.9579	0.9618	1.0024	0.901	0.9635
T12 (p.u.)	0.9	1.1	0.9283	0.9122	0.9737	0.9012	0.9693	0.9055	0.9451
T15 (p.u.)	0.9	1.1	1.0223	0.9907	1.0691	0.9633	1.0402	0.9044	0.9791
T36 (p.u.)	0.9	1.1	0.9709	0.9616	0.9162	0.9315	0.9472	0.9041	0.9423
QC10 (MVAr)	0	0.05	0.0498	0.0496	0.0308	0.049	0.0337	0.0488	0.041
QC24 (MVAr)	0	0.05	0.0499	0.0486	0.0374	0.0499	0.0489	0.0481	0.044
H5 (MWth)	10	35	34.7409	26.9466	34.004	15.5914	34.9802	10.2603	31.7985
H8 (MWth)	10	35	34.9596	11.6917	29.9034	31.013	26.5076	25.0408	21.4362
H11 (MWth)	10	35	34.8046	16.6686	30.7644	12.3085	34.5312	20.1664	22.0741
H13 (MWth)	20	35	34.9983	34.3144	34.0443	33.6069	33.6609	31.4813	31.0348
H31 (MWth)	0	2695.2	35.4967	85.3788	46.2839	82.4802	45.3202	88.0512	68.6565
Thermal cost ($/h)			14 554.4097	18 496.6161	14 774.2142	18 571.3435	15 866.5299	17 513.8138	18 023.2259
Emission (t/h)			0.4132	0.2059	0.3885	0.2071	0.3797	0.2264	0.2131
Carbon tax ($/h)			8.264	4.118	7.77	4.142	7.594	4.528	4.262
Ploss (MW)			10.18	3.37	10.58	3.27	11.06	4.5	4.61
VD (p.u.)			1.247	1.108	0.5545	1.1323	0.1644	2.6615	0.1679
L-index			0.1333	0.1361	0.1363	0.1342	0.146	0.1152	0.1454

Table 6
Simulation results and control parameters of different cases for CHPED based OPF using CDTBO.

Control parameters	Min.	Max.	Case 1	Case 2	Case 3	Case 4	Case 5	Case 6	Case 7
PTG1 (MW)	50	200	191.51	64.9	183.6	55.86	127.91	85.41	58.28
PTG2 (MW)	20	80	52	68.03	54.28	76.42	77.4	77.86	79.33
PTG5 (MW)	15	50	15.23	49.88	15.12	49.68	48.46	48.49	49.99
PTG8 (MW)	10	35	11.35	34.27	11.54	34.83	15	34.99	34.29
PTG11 (MW)	10	30	11.49	30	13.09	29.95	12.52	28.78	29.79
PTG13 (MW)	12	40	12.02	39.53	16.61	39.82	12.02	12.32	36.45
V1 (p.u.)	0.95	1.1	1.098	1.0904	1.0495	1.0693	0.9765	1.0983	0.9826
V2 (p.u.)	0.95	1.1	1.0854	1.0844	1.0234	1.0647	1.026	1.0985	0.9837
V5 (p.u.)	0.95	1.1	1.0553	1.0664	1.0017	1.0439	1.0138	1.0951	0.9985
V8 (p.u.)	0.95	1.1	1.0646	1.0746	1.0058	1.052	1.0126	1.0984	1.0242
V11 (p.u.)	0.95	1.1	1.0987	1.0919	1.0847	1.0996	1.0456	1.097	1.0783
V13 (p.u.)	0.95	1.1	1.0975	1.0955	1.0522	1.0992	1.0533	1.0999	1.0588
T11 (p.u.)	0.9	1.1	1.0528	1.0521	1.0524	1.0021	1.0129	0.908	1.0631
T12 (p.u.)	0.9	1.1	0.9045	0.9054	0.9281	0.9022	0.9052	0.9015	0.9016
T15 (p.u.)	0.9	1.1	1.0203	1.0154	1.0449	0.9787	1.0119	0.9034	1.0203
T36 (p.u.)	0.9	1.1	0.9724	0.9763	0.9923	0.9483	0.9492	0.9032	0.9475
QC10 (MVAr)	0	0.05	0.0497	0.0486	0.0359	0.05	0.0393	0.0476	0.0453
QC24 (MVAr)	0	0.05	0.05	0.046	0.0427	0.0493	0.05	0.0488	0.05
H5 (MWth)	10	35	34.9757	19.1045	35.5515	22.0812	14.005	33.7118	34.9708
H8 (MWth)	10	35	34.7559	24.4885	34.6399	28.5276	25.4611	21.5057	31.5227
H11 (MWth)	10	35	34.4638	31.4853	34.8829	12.1995	32.0431	11.6057	27.0947
H13 (MWth)	20	35	34.6095	26.5912	34.8584	26.294	29.0664	34.3624	30.2508
H31 (MWth)	0	2695.2	36.1951	73.3305	35.0674	85.8977	74.4245	73.8144	51.161
Thermal cost ($/h)			14 552.5479	18 475.776	14 765.0941	18 574.8846	16 091.571	17 412.8286	18 304.9366
Emission (t/h)			0.413	0.2053	0.3862	0.2063	0.2752	0.2271	0.2088
Carbon tax ($/h)			8.26	4.106	7.724	4.126	5.504	4.542	4.176
Ploss (MW)			10.2	3.21	10.84	3.16	9.91	4.45	4.73
VD (p.u.)			1.2195	1.3002	0.3805	1.3554	0.1542	2.6902	0.1665
L-index			0.1336	0.1331	0.1544	0.1318	0.1462	0.1149	0.1454

$$+\left|\delta_{poui}\ Sin\ \left\{\varepsilon_{poui}\times\left(P_{poui}^{\min}-P_{poui}\right)\right\}\right| \tag{13}$$

Eq. (13) becomes more non-linear and non-differentiable due to sinusoidal terms from the quadratic equation and sinusoidal terms from the valve point loading. The ith unit's valve point effects coefficients are denoted by δ_{poui} and ε_{poui}; The cost function of heat-only units and co-generation units is defined by the equations in (14) and (15).

$$\begin{cases} Cost_{chpi}\left(P_{chpi},H_{chpi}\right)=\alpha_{chpi}\left(P_{chpi}\right)^2+\beta_{chpi}P_{chpi}+\gamma_{chpi} \\ +\delta_{chpi}\left(H_{chpi}\right)^2+\varepsilon_{chpi}H_{chpi}+\kappa_{chpi}H_{chpi}P_{chpi} \end{cases} \tag{14}$$

$$Cost_{houi}\left(H_{houi}\right)=\alpha_{houi}\left(H_{houi}\right)^2+\beta_{houi}H_{houi}+\gamma_{houi} \tag{15}$$

Table 7
Statistical analysis of test system 1.

Algorithm	Statistical analysis	Cost ($/h)	Emission (t/h)	Power loss (MW)	Voltage profile (pu)	Voltage stability (pu)
DTBO	Min	14 554.4097	0.2059	3.27	0.1644	0.1152
	Mean	14 560.1265	0.2066	3.34	0.1651	0.1158
	Max	14 575.7283	0.2072	3.55	0.1672	0.1178
CDTBO	Min	14 552.5479	0.2053	3.16	0.1542	0.1149
	Mean	14 558.6823	0.2058	3.21	0.1549	0.1151
	Max	14 564.2323	0.2065	3.33	0.1562	0.1162

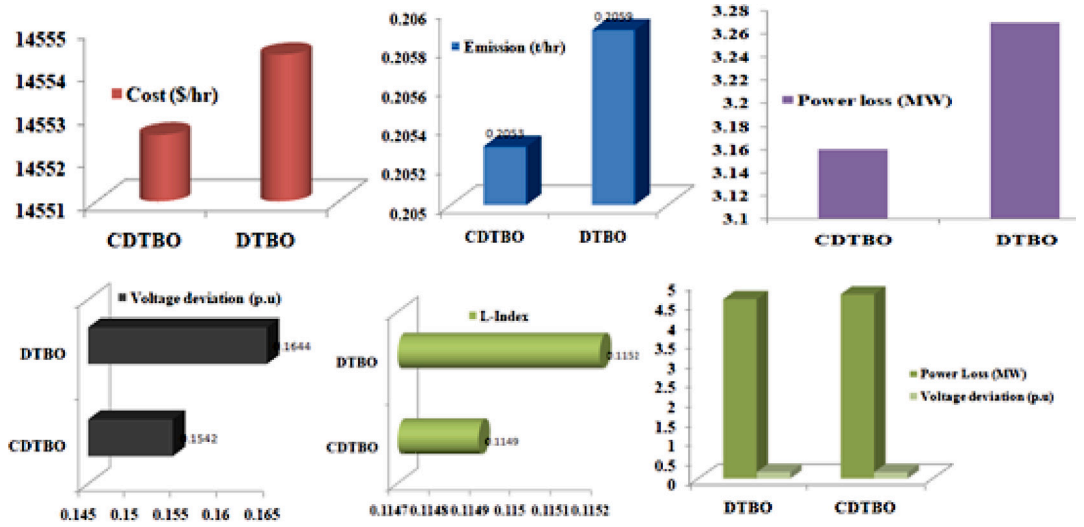

Fig. 5. Different comparison graphs of CHPED based OPF system.

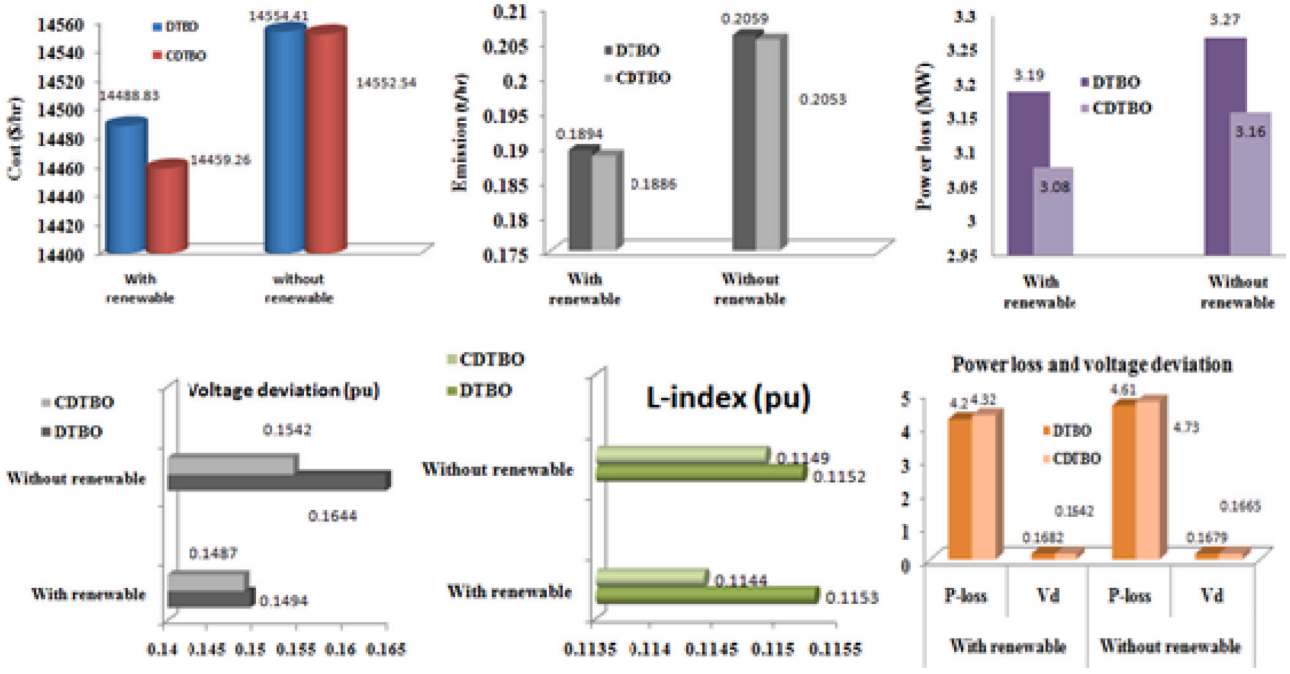

Fig. 6. Different comparison graphs of with and without renewable sources.

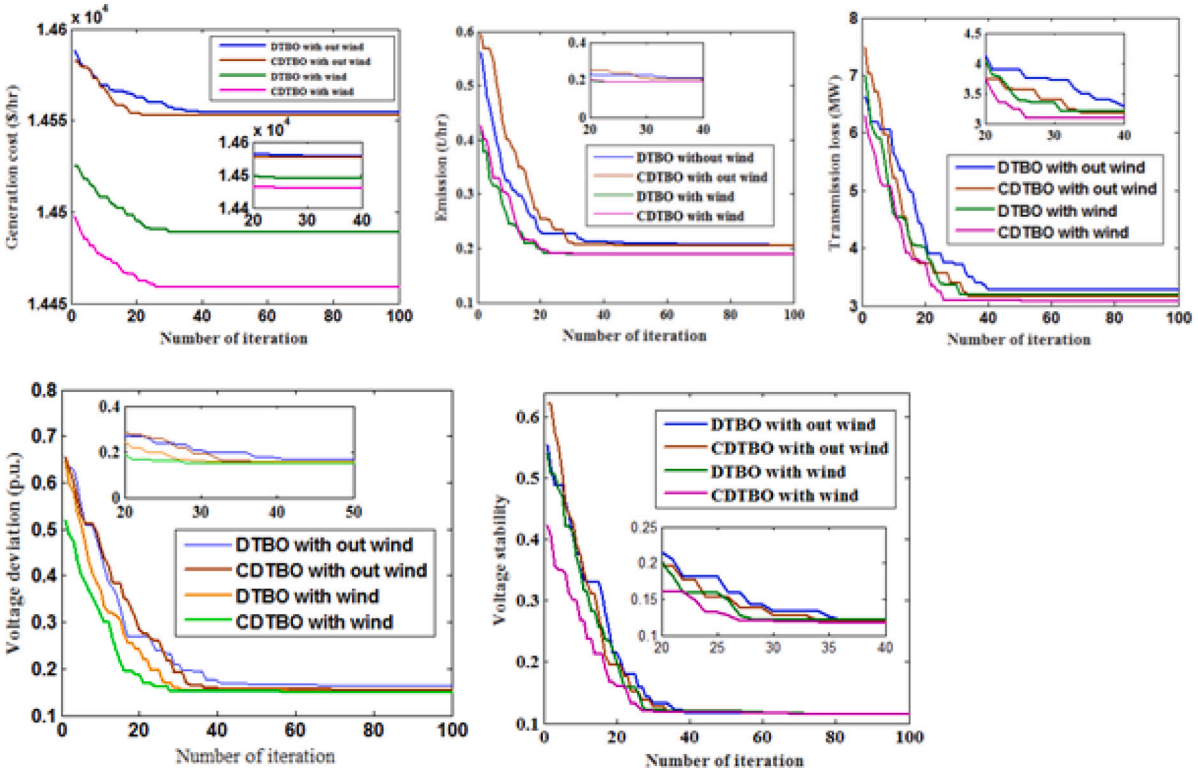

Fig. 7. Comparison of convergence graph of different objective functions.

Table 8
An outline of the IEEE 30 bus setup for wind-powered CHPED-OPF.

Items	Quantity	Details
Buses Branches	30 41	[ref] [ref]
Thermal generators (TG1,TG2,TG3,TG4,TG5)	3	2 power only units (buses 1, 2), 4 CHP units (buses 5, 8, 11 and 13) and 1 heats only unit
Wind generators (WG1)	1	Buses:2
Tap changing transformer	4	Branches:(6–9), (6–10), (4–12) and (27–28)
Control variables	11	Scheduled active power of 5Nos. Generators:TG2,TG3,TG4,TG5,WG1,; every generator bus's voltages (6Nos.) transformer tap setting and compensation devices
Load demand, Heat demand		283.4 MW, 126.2 MVAr,175 MWth
Range of load bus voltage Compensation devices	24 2	[0.95–1.05] p.u. Buses: 10 and 24

In above expression, $Cost_{chpi}\left(P_{chpi}, H_{chpi}\right)$ and $Cost_{houi}\left(H_{houi}\right)$ define the cost equation of the ith co-generation unit and heat only unit, respectively.

3.1.2. Case 2: CHPED based OPF with wind

The cost function of wind based CHPED problem is presented by (16).

$$Minimum\ Cost = \sum_{i=1}^{N_{pou}} Cost_{poui}\left(P_{poui}\right) + \sum_{i=1}^{N_{chp}} Cost_{chpi}\left(P_{chpi}, H_{chpi}\right) + \sum_{i=1}^{N_{hou}} Cost_{houi}\left(H_{houi}\right) + \sum_{i=1}^{N_{wind}} Cost_{windi}\left(P_{windi}\right) \quad (16)$$

In the above equation, $Cost_{windi}\left(P_{windi}\right)$ denotes the wind generation cost; number of wind units represented by N_{wind} respectively.

3.1.3. Emission minimization

The objective of the second single objective function is to minimize emissions without considering cost minimization. The thermal plant emission ($emission_{pou}$) is represented mathematically in Eq. (17).

$$Minimum\ emission_{pou} = \sum_{t=1}^{T}\sum_{i=1}^{N_{pou}}\left[b_{i0} + b_{i1}P_{poui}^{t} + b_{i2}(P_{poui}^{t})^{2} + b_{i3}\exp(b_{i4}P_{poui}^{t})\right] \quad (17)$$

In (17), b_{i0}, b_{i1}, b_{i2}, b_{i3} and b_{i4} denote emission coefficients whereas P_{poui}^{t} is the thermal power output.

3.1.4. Active power loss

Transmission lines experience active power loss due to inherent resistance. (18) shows the active power loss that has to be kept to a minimum:

$$P_L = \sum_{n=1}^{N_L} G_{n(pq)}\left(V_p^2 + V_q^2 - 2V_pV_q\cos\varphi_{pq}\right) \quad (18)$$

$G_{n(pq)}$: transfer conductance of nth line connected between buses p and q. N_L: total number of transmission line. ϕ_{pq}: voltage angle between buses p and q.

3.1.5. Voltage deviation

Voltage variation at load buses must be kept to a minimum in order to maintain a suitable voltage profile at the load buses; this is indicated by (19):

$$VD = \sum_{l=1}^{N_B}|V_l - 1| \quad (19)$$

Table 9
Simulation results and control parameters of different cases for CHPED based OPF with renewable using DTBO.

Control parameters	Min.	Max.	Case 8	Case 9	Case 10	Case 11	Case 12	Case 13	Case 14
PTG1 (MW)	50	200	169.27	62.22	169.7	59.16	101.66	103.37	65.49
PWG2 (MW)	0	75	72.62	72.16	73.41	74.96	74.45	69.94	70.1
PTG5 (MW)	15	50	15.3	47.88	15.04	48.49	49.28	42.4	49.49
PTG8 (MW)	10	35	11.47	34.69	11.65	34.85	24.16	32.3	34.81
PTG11 (MW)	10	30	12.16	29.94	11.53	30	27.4	28.87	29.57
PTG13 (MW)	12	40	12.08	39.8	12.23	39.13	12.43	12.03	38.15
V1 (p.u.)	0.95	1.1	1.0938	1.084	1.0596	1.0896	1.0054	1.0871	0.9985
V2 (p.u.)	0.95	1.1	1.0733	1.0768	1.0397	1.0854	1.0027	1.0999	1.0036
V5 (p.u.)	0.95	1.1	1.0423	1.0578	1.0035	1.067	1.02	1.0989	1.0094
V8 (p.u.)	0.95	1.1	1.0541	1.0617	1.0112	1.0732	1.0144	1.0969	1.0183
V11 (p.u.)	0.95	1.1	1.0926	1.0881	1.0937	1.0963	1.0198	1.0933	1.0462
V13 (p.u.)	0.95	1.1	1.0968	1.0989	1.0981	1.0952	1.0397	1.0998	1.0312
T11 (p.u.)	0.9	1.1	0.9862	1.0086	0.9923	1.0122	0.9929	0.9038	0.9656
T12 (p.u.)	0.9	1.1	0.9304	0.9192	0.9135	0.9541	0.9022	0.9048	0.961
T15 (p.u.)	0.9	1.1	1.0088	1.0073	1.0046	1.0115	0.9822	0.9028	0.9702
T36 (p.u.)	0.9	1.1	0.9467	0.9612	0.9441	0.981	0.9444	0.9031	0.9441
QC10 (MVAr)	0	0.05	0.047	0.0498	0.0476	0.0497	0.0478	0.0411	0.0475
QC24 (MVAr)	0	0.05	0.05	0.0485	0.0483	0.0495	0.0494	0.0474	0.0499
H5 (MWth)	10	35	34.5514	11.804	34.1251	32.3734	11.9037	29.3479	15.5953
H8 (MWth)	10	35	34.7341	27.4446	34.9951	11.306	12.9738	10.8335	22.9548
H11 (MWth)	10	35	34.6469	13.3893	34.7639	14.64	24.0739	13.3333	27.4824
H13 (MWth)	20	35	34.9519	22.1064	34.1294	21.9904	29.7466	29.3231	30.3763
H31 (MWth)	0	2695.2	36.1157	100.2557	36.9865	94.6902	96.302	92.1622	78.5912
Thermal cost ($/h)			14 488.8256	18 464.4101	14 471.7058	18 439.7017	16 989.6891	17 030.7502	18 338.5572
Emission (t/h)			0.3385	0.1894	0.3397	0.1886	0.221	0.2222	0.1906
Carbon tax ($/h)			6.77	3.788	6.794	3.772	4.42	4.444	3.812
Ploss (MW)			9.5	3.28	10.16	3.19	5.98	5.51	4.2
VD (p.u.)			1.2745	1.308	0.6885	1.289	0.1494	2.6469	0.1682
L-index			0.1315	0.1325	0.1397	0.1339	0.1462	0.1153	0.1459

Table 10
Simulation results and control parameters of different cases for CHPED based OPF with renewable using CDTBO.

Control parameters	Min.	Max.	Case 8	Case 9	Case 10	Case 11	Case 12	Case 13	Case 14
PTG1 (MW)	50	200	167.82	59.59	168.3	58.09	96.93	87.51	61.98
PWG2 (MW)	0	75	74.71	73.85	74.13	74.39	72.54	74.33	74.1
PTG5 (MW)	15	50	15.08	49.61	15.18	49.62	49.76	48.85	48.89
PTG8 (MW)	10	35	11.77	33.63	11.4	34.6	28.33	34.86	34.01
PTG11 (MW)	10	30	11.26	29.97	11.66	29.93	29.28	29.72	29.5
PTG13 (MW)	12	40	12.11	39.92	12.05	39.85	12.43	12.61	39.24
V1 (p.u.)	0.95	1.1	1.097	1.0942	1.0993	1.0971	1.0011	1.0989	0.9929
V2 (p.u.)	0.95	1.1	1.0849	1.0884	1.0878	1.0945	1.0016	1.0995	0.9965
V5 (p.u.)	0.95	1.1	1.0486	1.0676	1.057	1.0743	1.0166	1.0992	1.0173
V8 (p.u.)	0.95	1.1	1.0613	1.0721	1.0635	1.0832	1.0235	1.0998	1.0099
V11 (p.u.)	0.95	1.1	1.097	1.1	1.0918	1.0996	0.9829	1.0984	1.0529
V13 (p.u.)	0.95	1.1	1.0996	1.0989	1.0982	1.0993	1.0448	1.0997	1.0552
T11 (p.u.)	0.9	1.1	1.0383	0.992	1.0362	1.044	0.9623	0.9057	0.9771
T12 (p.u.)	0.9	1.1	0.9013	0.9754	0.9051	0.9016	0.9037	0.9024	0.942
T15 (p.u.)	0.9	1.1	1.012	1.0129	1.0193	0.9999	0.9869	0.9014	1.0145
T36 (p.u.)	0.9	1.1	0.9646	0.9853	0.9705	0.9731	0.9448	0.9016	0.9424
QC10 (MVAr)	0	0.05	0.0488	0.0494	0.0498	0.0499	0.0469	0.0498	0.046
QC24 (MVAr)	0	0.05	0.0498	0.0481	0.0488	0.0494	0.0476	0.0478	0.0489
H5 (MWth)	10	35	34.914	22.2784	34.9677	15.691	22.336	17.6832	16.2992
H8 (MWth)	10	35	34.6553	28.1458	34.7792	17.4928	14.0736	11.6333	23.9166
H11 (MWth)	10	35	34.9839	13.1031	34.9659	29.1142	12.2997	32.6136	13.3693
H13 (MWth)	20	35	34.884	33.8426	34.9655	24.442	26.3268	30.0584	34.159
H31 (MWth)	0	2695.2	35.5628	77.6301	35.3217	88.2599	99.9639	83.0115	87.2558
Thermal cost ($/h)			14 459.2598	18 379.6367	14 462.0813	18 463.134	17 256.6276	17 395.1858	18 369.8968
Emission (t/h)			0.3355	0.1886	0.3365	0.1882	0.2162	0.2088	0.1895
Carbon tax ($/h)			6.71	3.772	6.73	3.764	4.324	4.176	3.79
Ploss (MW)			9.36	3.17	9.32	3.08	5.87	4.48	4.32
VD (p.u.)			1.276	1.3139	1.2502	1.5747	0.1487	2.7396	0.1642
L-index			0.1327	0.1343	0.1333	0.13	0.1458	0.1144	0.1461

3.1.6. L-index

It is essential to keep each bus's bus voltage constant and suitable throughout normal operation. In this work, voltage stability is improved by minimizing the voltage stability indicator L-index. The indicator values, with minor adjustments, range from 0 to 1. Here is a quick rundown of what the L-index of a power system means. In a multi-node system, the following can be used to explain the voltage and current between the load and generator buses (20).

$$\begin{bmatrix} I_{l'} \\ I_{g'} \end{bmatrix} = \begin{bmatrix} y_{l'l'} & y_{l'g'} \\ y_{g'l'} & y_{g'g'} \end{bmatrix} \begin{bmatrix} V_{l'} \\ V_{g'} \end{bmatrix} \tag{20}$$

Table 11
Statistical analysis of test system 2.

Algorithm	Statistical analysis	Cost ($/h)	Emission (t/h)	Power loss (MW)	Voltage profile (pu)	Voltage stability (pu)
DTBO	Min	14 488.8256	0.1894	3.19	0.1494	0.1153
	Mean	14 495.2315	0.1902	3.26	0.1504	0.1162
	Max	14 508.7845	0.1915	3.38	0.1521	0.1179
CDTBO	Min	14 459.2598	0.1886	3.08	0.1487	0.1144
	Mean	14 464.0213	0.1891	3.1	0.1494	0.1147
	Max	14 469.6412	0.1899	3.25	0.1512	0.1152

Table 12
Comparison of different optimal single objective results for test system 1 and test system 2 using CDTBO.

CDTBO	Cost ($/h)	Emission (t/h)	Power loss (MW)	Voltage profile (pu)	Voltage stability (pu)
With renewable	14 459.26	0.1886	3.08	0.1487	0.1144
Without renewable	14 552.55	0.2053	3.16	0.1542	0.1149

By matrix inversion, the above equation may be rearranged as follows (21):

$$\begin{bmatrix} V_{l'} \\ I_{g'} \end{bmatrix} = \begin{bmatrix} Z_{l'l'} & F_{l'g'} \\ K_{g'l'} & Y_{g'g'} \end{bmatrix} \begin{bmatrix} I_{l'} \\ V_{g'} \end{bmatrix} \tag{21}$$

The sub-matrix $F_{l'g'}$ may be expressed as under (22):

$$F_{l'g'} = -\left[y_{11}\right]^{-1} \left[y_{l'g'}\right] \tag{22}$$

The voltage stability index of the Kth bus may be expressed by (23).

$$L_k = |1 - \sum_{j=1}^{Ng} F_{kj} \frac{V_j}{V_k} | k = 1, 2, \ldots ..., N_l \tag{23}$$

3.1.7. Multi-objective function

Functions that were formerly single-objective are minimized separately. On the other hand, to evaluate the recommended method's efficacy in a multi-objective setting, active power losses and voltage variation are minimized concurrently following the first simultaneous minimization of generating cost and emission. In order to equalize the priority level of the generation cost with emission and power losses with voltage deviation, a penalty factor (ϵ) has been used to handle the multi-objective function. The mathematical representation of the multi-objective function (F) is formulated in (24) and (25).

$$F = (MinimumCost) + \epsilon\,(Minimumemission) \tag{24}$$

$$F = (P_L) + \epsilon\,(V\,D) \tag{25}$$

3.2. Constraints

3.2.1. Equality constraints

The following illustration shows the limitations of both CHPED-based OPF and CHPED-based OPF with wind.

3.2.1.1. Power balance constraints of for without renewable. The following are the power balancing restrictions for the OPF system based on CHPED:

$$\sum_{i=1}^{N_{pou}} P_{poui} + \sum_{i=1}^{N_{chp}} P_{chpi} = P_D + P_L \tag{26}$$

$$P_L = \sum_{i=1}^{N_{pou}} \sum_{j=1}^{N_{pou}} P_{poui} B_{ij} P_{pouj} + \sum_{i=1}^{N_{pou}} \sum_{j=1}^{N_{chp}} P_{poui} B_{ij} P_{chpj} + \sum_{i=1}^{N_{chp}} \sum_{j=1}^{N_{chp}} P_{chpi} B_{ij} P_{chpj} \tag{27}$$

$$\sum_{i=1}^{N_{chp}} H_i + \sum_{i=1}^{N_h} H_{chpi} = H_D \tag{28}$$

Eq. (26) representation of power balance; power losses in the transmission line shown in Eq. (27); Eq. (28) represents heat balance. thermal demand defined by H_D and B_{im}, B_{ij}, B_{jr} are power loss coefficients.

3.2.1.2. Power balance constraints for with renewable system. The wind power balance equation for CHPED-based OPF is defined by (29):

$$\sum_{i=1}^{N_{pou}} P_{poui} + \sum_{i=1}^{N_{chp}} P_{chpi} + \sum_{i=1}^{N_{wind}} P_{windi} = P_D + P_L \tag{29}$$

The power balance Eq. (26) is extended to a new solution as represented in (29), where wind power is incorporated with CHPED.

Power flow equation is shown in Eq. (30):

$$\begin{cases} \sum_{c=1}^{N_s} \left(P_{Gc} - P_{Lc}\right) = \sum_{c=1}^{N_s} \sum_{d=1}^{N_s} |V_c|\,|V_d|\,|Y_{cd}| \cos\left(\varphi_{cd} - \beta_{cd}\right) \\ \sum_{c=1}^{N_s} \left(Q_{Gc} - Q_{Lc}\right) = -\sum_{c=1}^{N_s} \sum_{d=1}^{N_s} |V_c|\,|V_d|\,|Y_{cd}| \sin\left(\varphi_{cd} - \beta_{cd}\right) \end{cases} \tag{30}$$

In the cth bus, the active and reactive power demand are denoted by P_{Lc} and Q_{Lc}; the active and reactive power of generation and demand are denoted by P_{Gc} and Q_{Gc}, respectively; The transmission line admittance between the cth and the dth bus is Y_{cd}; the number of buses is N_s; the admittance angle between the cth and the dth bus is φ_{cd}.

3.2.2. Constraint of inequality

3.2.2.1. Constraints of capacity. For stable operation, the heat and power limitation range for power alone units, co-generation units, and heat only units is provided in (31)–(35). The co-generation and power unit voltages are shown in (36)–(37). (38)–(40) provide the constraints of transformer tap changers, load buses, and transmission lines. :

$$P_{poui}^{\min} \le P_{poui} \le P_{poui}^{\max}\, where, i = 1, 2, 3, \ldots, N_{pou} \tag{31}$$

$$P_{chpi}^{\min}\left(H_{chpi}\right) \le P_{chpi} \le P_{chpi}^{\max}\left(H_{chpi}\right)\, where, i = 1, 2, 3, \ldots, N_{chp} \tag{32}$$

$$P_{windi}^{\min} \le P_{windi} \le P_{windi}^{\max}\, where, i = 1, 2, 3, \ldots, N_{wind} \tag{33}$$

$$H_{chpi}^{\min}\left(P_{chpi}\right) \le H_{chpi} \le H_{ci}^{\max}\left(P_{chpi}\right)\, where, i = 1, 2, 3, \ldots, N_{chp} \tag{34}$$

$$H_{houi}^{\min} \le H_{houi} \le H_{houi}^{\max}\, where, i = 1, 2, 3, \ldots, N_{hou} \tag{35}$$

$$V_{poui}^{\min} \le V_{poui} \le V_{poui}^{\max}\, where, i = 1, 2, 3, \ldots, N_{pou} \tag{36}$$

$$V_{chpi}^{\min} \le V_{chpi} \le V_{chpi}^{\max}\, where, i = 1, 2, 3, \ldots, N_{chp} \tag{37}$$

Table 13
Comparison optimal results of multi-objective functions for test system 1 and test system 2 using CDTBO.

Optimization	Multi-objective functions	With renewable		Without renewable	
CDTBO	Cost and Emission	Cost 14 462.08 ($/h)	Emission 0.3365 (t/h)	Cost 14 765.09($/h)	Emission 0.3862 (t/h)
	Active power loss and Voltage profile	Power loss 4.32 (MW)	Voltage profile 0.1642 (p.u)	Power loss 4.73 (MW)	Voltage profile 0.1665 (p.u)

Table 14
Comparison of different optimal single objective results for test system2 using different algorithm.

Algorithm	Cost ($/h)	Emission (t/h)	Power loss (MW)	Voltage profile (p.u)	Voltage stability (p.u)
CDTBO	14 459.26	0.1886	3.08	0.1487	0.1144
AFDB-ARO [40]	14 676.56	0.1954	3.54	0.1589	0.1207
dFDB-SFS [42]	14 623.78	0.1923	3.44	0.1556	0.1204
FDB-AGSK [43]	14 589.98	0.1907	3.32	0.1549	0.1198
FDB-TLABC [44]	14 577.45	0.1902	3.31	0.1535	0.1189
FDB-AEO [45]	14 534.09	0.1899	3.26	0.1512	0.1181
FDB-LFD [46]	14 523.78	0.1898	3.24	0.1509	0.1176
FDB-AGDE [47]	14 502.98	0.1895	3.21	0.1502	0.1166
LRFDB-COA [48]	14 526.89	0.1911	3.41	0.1513	0.1187
FDB-SFS [49]	14 543.98	0.1912	3.47	0.1533	0.1191
FDB-CHOA [50]	14 489.32	0.1891	3.19	0.1499	0.1167

(ii) Load bus constraints:

$$V_{Lb}^{\min} \le V_{Lb} \le V_{Lb}^{\max} \quad b \in N_{BL} \tag{38}$$

(iii) Transmission line constraints:

$$S_{Lb} \le S_{Lb}^{\max} \quad b \in N_{LT} \tag{39}$$

(iv) Transformer tap constraints:

$$T_b^{\min} \le T_b \le T_b^{\max} \quad b \in N_T \tag{40}$$

Minimum and maximum power limits of ith power only unit and ith co-generation unit are presented by $P_{poui}^{\min}$, $P_{poui}^{\max}$, $P_{chpi}^{\min}\left(H_{chpi}\right)$ and $P_{chpi}^{\max}\left(H_{chpi}\right)$; $P_{windi}^{\min}$ is the minimum power generation of ith wind $P_{windi}^{\max}$ is presented maximum power generation of ith wind, $H_{chpi}^{\min}$ and $H_{houi}^{\min}$ are the minimum heat limit of the ith co-generation and heat unit; $H_{chpi}^{\max}$ and $H_{houi}^{\max}$ are depicted the maximum heat limit of the ith co-generation heat unit.

where $V_{Gb}^{\min}, V_{Gb}^{\max}$indicate respectively lower and upper voltage limits, for the bth generator bus; $P_{Gb}^{\min}, P_{Gb}^{\max}$ are the lower and upper bounds of active power generation, respectively, of the bth bus; $Q_{Gb}^{\min}, Q_{Gb}^{\max}$ are respective minimum and maximum reactive power generation margins of the bth bus; $V_{Lb}^{\min}, V_{Lb}^{\max}$ are the smallest and highest voltage edges, respectively, of the bth load bus, ${S_{Lb}}^{\min}$, $S_{Lb}^{\max}$ are the least apparent power flow and extreme apparent power flow limit, respectively, of the $b$thbranch; $T_b^{\min}$, $T_b^{\max}$ are the bottom and extreme tap setting limits, respectively, of the bth regulating transformer; respectively.

4. Algorithm for optimization

4.1. Driving training optimization (DTBO)

Dehghani et al. introduces DTBO [51]. The DTBO program is designed to resemble the driving teacher training program used by driving centers. The DTBO mathematical framework consists of three phases: (1) student practice; (2) student patterning from instructor skills; and (3) driving instructor training. In order to be trained and get the ability to drive, a beginner's intelligence is required during the driving training procedure. A learner driver at a driving school has access to multiple instructors for instruction. Through practice and adhering to the instructor's instructions, a student improves his driving skills. The foundation of mathematical modeling of DTBO is these learner-teacher interactions and self-practice for improving driving skills. A population based meta-heuristic technique is called DTBO. Here is a representation of the DTBO population matrix (41), where each row member stands for a possible solution to the given problem:

$$Z = \begin{bmatrix} Z_1 \\ \vdots \\ Z_p \\ \vdots \\ Z_N \end{bmatrix}_{N\times m} = \begin{bmatrix} z_{11} & \cdots & z_{1q} & \cdots & z_{1m} \\ \vdots & \cdots & \vdots & \cdots & \vdots \\ z_{p1} & \cdots & z_{pq} & \cdots & z_{pm} \\ \vdots & \cdots & \vdots & \cdots & \vdots \\ z_{N1} & \cdots & z_{Nq} & \cdots & z_{Nm} \end{bmatrix}_{N\times m} \tag{41}$$

Z is the DTBO population, Z_p. is the pth member of the population *i.e.* pth candidate solution of the problem, z_{pq} is the qth variable of the pth solution of the problem, N is population size, m denotes no of problem variables. At the beginning of DTBO implementation, the starting position of DTBO members (*i.e.* candidate solutions) is initialized randomly as given below (42):

$$z_{pq} = z_{pq}^{\min} + r * \left(z_{pq}^{\max} - z_{pq}^{\min}\right) \quad for\ p = 1\ to\ N \quad \varsigma \quad q = 1\ to\ m \tag{42}$$

where $z_{pq}^{\max}$, $z_{pq}^{\min}$ are the upper and lower limit, respectively, of the qth variable of the considered problem; r is a unbiased random value within 0 and 1. For every individual candidate solution, the value of the objective function is computed and it is represented as follows (43):

$$F = \begin{bmatrix} F_1 \\ \vdots \\ F_p \\ \vdots \\ F_N \end{bmatrix}_{N\times 1} = \begin{bmatrix} F\left(Z_1\right) \\ \\ F\left(Z_p\right) \\ \\ F\left(Z_N\right) \end{bmatrix}_{N\times 1} \tag{43}$$

The objective function's computed values serve as the primary criterion for evaluating the merits of the solutions under consideration. Best member is determined by selecting the candidate solution that yields the highest objective function value. The best member is updated as the iteration moves forward. The three phases that comprise the updating of a candidate solution in DTBO are as follows:

Step 1: Driving teacher training (Exploration) The best members of DTBO are selected as a driving instructors, while the remaining members are classified as trainee drivers. Choosing the right instructors and developing their skills gives us the ability to look globally to find the best location for DTBO. The L number (45) of DTBO members is selected as instructors in each iteration based on a comparison of the objective function values. These instructors are represented as the driving matrix DI (44)

Table 15
Statistical comparison (5 trials) among various algorithms for IEEE 30 bus system-2 for case-8 (Friedman test).

Sample	CDTBO	DTBO	AFDB-ARO [40]	dFDB-SFS	FDB-AGSK [43]	FDB-TLABC [44]	FDB-AEO [45]	FDB-LFD [46]	FDB-AGDE [47]	LRFDB-COA [48]	FDB-SFS [49]	FDB-CHOA [50]
1	14 459.26	14 488.8256	14 676.56	14 623.78	14 589.98	14 577.45	14 534.09	14 523.78	14 502.98	14 526.89	14 543.98	14 489.32
2	14 465.345	14 496.234	14 680.67	14 633.562	14 590.324	14 579.672	14 537.982	14 528.891	14 511.403	14 539.453	14 544.459	14 490.564
3	14 476.345	14 489.324	14 686.98	14 625.908	14 594.234	14 582.783	14 544.234	14 532.562	14 523.647	14 529.676	14 550.673	14 494.654
4	14 471.435	14 499.209	14 677.87	14 635.911	14 599.452	14 592.782	14 548.381	14 539.564	14 509.562	14 531.453	14 548.982	14 502.003
5	14 462.234	14 495.756	14 685.821	14 624.426	14 601.452	14 580.002	14 550.038	14 525.395	14 507.329	14 532.067	14 544.521	14 494.871

as follows:

$$DI = \begin{bmatrix} \begin{Bmatrix} DI_1 \\ . \\ . \\ DI_p \\ \\ DI_L \end{Bmatrix}_{L\times m} = \begin{bmatrix} \begin{Bmatrix} DI_{11} & . & . & DI_{1q} & . & DI_{1m} \\ . & . & & . & . & . \\ & . & & . & . & . \\ DI_{p1} & . & . & DI_{pq} & . & DI_{pm} \\ . & . & & . & . & . \\ . & . & & . & . & . \\ DI_{L1.} & . & . & DI_{Lq} & . & DI_{Lm} \end{Bmatrix}_{L\times m} \end{bmatrix} \tag{44}$$

DI_p is pth driving instructor. DI_{pq} is qth variable of pth instructor.

$$L = \left\lfloor 0.1 \times N \times \left(\frac{1-s}{S}\right) \right\rfloor \tag{45}$$

s denotes current iteration and S is maximum iteration. In this step, the modified position of DTBO population member is obtained as given below (46):

$$z_{pq}^{st1} = \begin{Bmatrix} \begin{Bmatrix} z_{pq} + r.\left(DI_{kpq} - I.z_{pq}\right), & F_{DIk_p} < F_p \\ z_{pq} + r.\left(z_{pq} - DI_{kpq}\right), & otherwise \end{Bmatrix} \end{Bmatrix} \tag{46}$$

Using Eq. (47), previous position is replaced by new position while it improves the objective function value.

$$Z_p = \begin{Bmatrix} \begin{Bmatrix} Z_p^{st1}, & F_p^{st1} < F_p \\ Z_p, & otherwise \end{Bmatrix} \end{Bmatrix} \tag{47}$$

Z_p^{st1} is newly computed pth candidate solution at step 1 of DTBO, z_{pq}^{st1} is its qth problem variable, F_p^{st1} is its objective function value, I is a random number in the set 1,2, r is random value within 0 and 1. In DI_{kpq}, k is randomly selected from the set $1, 2, \ldots., L$ *i.e.* kth driving instructor and F_{DIk_p} is its objective function value, p indicates pth member of the population which is being trained by kth instructor.

Step 2: Student driver's teacher skill patterning (Exploration) In the second step, student drivers mimic the instructor's actions and abilities to enhance the DTBO solution. Members of DTBO travel to various regions of the search space through this process. It amplifies the exploratory power of DTBO. A modified position is established through a linear combination between the teachers and DTBO members; this combination is described mathematically by Eq. (48). If the value of the objective function is better than the previous position, the new position is substituted using Eq. (49).

$$z_{pq}^{st2} = \xi.z_{pq} + (1-\xi).DI_{kpq} \tag{48}$$

$$Z_p = \begin{Bmatrix} \begin{Bmatrix} Z_p^{st2}, & F_p^{st2} < F_p \\ Z_p, & otherwise \end{Bmatrix} \end{Bmatrix} \tag{49}$$

Z_p^{st2} is the modified pth candidate solution on second stage of DTBO, z_{pq}^{st2} is its qth variable, F_p^{st2} is corresponding value of objective function. ξ is called patterning index described by Eq. (50):

$$\xi = 0.01 + 0.9\left(1 - \frac{s}{S}\right) \tag{50}$$

Step 3: Personal practice (Exploitation) Based on individual practice, the novice drivers' driving abilities are improved in this level. It is comparable by using DTBO's local search power. Every learner looks for a position that is better than their current one. Eq. (51) is used to generate new placements in close proximity to the existing position. The prior position is replaced with Eq. (52) if the new position increases the objective function value more than the previous one did.

$$z_{p,q}^{st3} = z_{pq} + (1-2r).R.\left(1 - \frac{s}{S}\right).z_{pq} \tag{51}$$

$$Z_p = \begin{Bmatrix} \begin{Bmatrix} Z_p^{st3}, & F_p^{st3} < F_p \\ Z_p, & otherwise \end{Bmatrix} \end{Bmatrix} \tag{52}$$

Z_p^{st3} is the updated pth candidate solution at third step of DTBO, $z_{p,q}^{st3}$ is its qth variable, corresponding objective function value is F_p^{st3}, r is a random value between 0 and 1, R is 0.05, s is current iteration and S is the maximum iteration. One DTBO iteration is finished when all population members are updated through steps 1–3. Following that, the following iteration begins with a newly updated population, and so on [through Eqs. (44) to (52)] until the last iteration is finished. The problem's best candidate solution is noted as the solution at the conclusion of the last iteration.

4.2. Chaotic based learning (CBL)

Most of the evolutionary algorithms learn from the population's random initialization and continuous search for the optimal solution. But, when it comes to find the global optimal solution, which also affects the rate of convergence, DTBO still cannot compete with other techniques. To mitigate this effect, chaos behavior and the DTBO are combined to generate the CDTBO. Chaos's unpredictable and non-repeating characteristics make overall searches speedier, which can be essential for quickening the convergence of a meta-heuristic algorithm.

In the CDTBO approach, various chaotic maps are merged with DTBO to adjust the parameters of DTBO. Ten chaotic maps with varying behaviors make up the chaotic set combination. The starting value for the ideal solution is chosen to be 0.7 in the range of 0 to 1. Table 1 discusses the various chaotic maps, and Table 2 shows the statistical analysis of the CDTBO technique for various chaotic maps. By employing these chaotic maps, the local optimal problem has been solved and a global optimal solution is provided.

4.3. Solving OPF-CHPED issue by CDTBO

In order to improve the optimizing efficiency, DTBO and CBL are combined in this article (referred to as CDTBO). The CDTBO algorithm's flow chart is shown in Fig. 2, and the steps it takes to apply to OPF are described below :

Step 1: Create the initial population Z at random. Z stands for the independent variables of the OPF issue, which include tap settings for regulating transformers, the active powers of all generators (slack bus excluded) & load voltages . Z shouldn't go against the restrictions on inequality & equality.

Step 2: The chaotic map is used to initialize the random value. The chaotic number is modified with the aid of the chaotic map equation.
Step 3: Carry out load flow by Newton–Raphson (NR) procedure [52] & compute full dependent variables like load voltages, slack bus active power etc from Z.
Step 4: Determine the magnitudes of objective function for Z.
Step 5: Assemble the population Z from finest to worst according to magnitude of the objective function.
Step 6: Create N number of best possible fit members from Z.
Step 7: Start DTBO
Step 8: Training by the driving instructor (Exploration)
Step 9: Comparing the objective function's value, acquire the driving instructor matrix DI.
Step 10: Select a driving instructor randomly from DI matrix.
Step 11: By Eq. (46), get the new position for pth DTBO member.
Step 12: Use the NR procedure to confirm whether the limitations are within the allowed bounds.
Step 13: By Eq. (47), the position of pth DTBO member is enhanced. Patterning of the instructor skills of the student driver (Exploration)
Step 14: Through Eq. (50), find the patterning index.
Step 15: Compute a new position for pth DTBO member by Eq. (48).
Step 16: Check if the constraints are within the limits or not by NR process.
Step 17: Use Eq. (49), to update the position of pth DTBO member.
Step 18: Personal practice (Exploitation)
Step 19: Compute the updated position of pth DTBO member with Eq. (51).
Step 20: Verify using the NR process whether the constraints are within the allowed bounds
Step 21: By Eq. (52), to revise the position of pth DTBO member.
Step 22: Following the creation of new populations using DTBO, feasible solutions based on CBL are produced, and the fitness value is assessed
Step 23: From the DTBO and CBL based solutions, the required number of workable solutions is chosen.
Step 24: For the subsequent iteration, proceed to step 5 until the halting criterion is met.
Step 25: Output: The best candidate solution achieved by CDTBO.

5. Simulation results

In the current work, CHPED is integrated with the IEEE 30 bus system for optimal power flow in the transmission line with the best possible objective function solution. The CHPED-OPF problem of the power system is now being investigated through simulation using two test systems. The CDTBO algorithms are used to find optimal answers on the considered test systems, and the test results show how effective and beneficial the algorithm is. In order to solve the CHPED-OPF problem, the performances of CDTBO and DTBO are contrasted. It demonstrates CDTBO's superiority. The simulations are done in MATLAB 2014. The PC used to run MATLAB is powered by a more recent Core i5 CPU with internal memory 8 GB of RAM & 2.5 GHz. The simulation results and calculation times for test systems 1 & 2 of the proposed algorithm are shown in this section. The practical and realistic range within which the power and heat production of the different co-generation units falls is also explained. At population size 50, the CDTBO algorithm produces the best outcomes in the lowest amount of time. For every population and case, there are 100 iterations. Furthermore, CDTBO has been applied in test systems that take renewable sources into account as well as those that do not. Comparison is made between the simulation results of CDTBO and DTBO for test systems with renewable energy sources. The fourteen different cases involving single and multi-objective functions that are looked at in this research are listed in Table 3. According to the simulation results, utilizing renewable energy sources reduces generation costs when compared to OPF-CHPED systems that rely on non-renewable energy.

5.0.1. Test system-1

Having 30 buses, test system 1 is made up of a heat, four CHP, & two power units. 41 branches are there through that 30 buses are linked. Bus no 5, 8, 11 & 13 are being fitted with CHP units and two power units are linked to bus no 1 & 2. There is 283.4 MW of load demand in total, the reactive power & heat demand are 126.2 MVar & 175 MWth. Six reactive powers, six total generator bus voltages, four tap-varying transformers, & five heat-only units are considered under the control variables. On 24 load buses, the voltage is found within 0.95 & 1.05 p.u. An outline of IEEE 30 bus for OPF-CHPED structure is given in Table 4. Co-generation units' competence to generate both power & heat located in viable operating area are displayed at Figs. 3 and 4. There have been seven cases for single and multi-objective functions tested on the suggested test system 1. The functions having single objective contain minimizing overall cost, emissions, transmission loss, voltage profile & L-index. The functions with multi-objectives enclose minimizing cost with emission and active power loss with voltage profile concurrently. Applying DTBO the computed optimal cost is 14554.41 $/h, emission 0.2059 (t/h), carbon tax is 4.118 ($/h), transmission losses is 3.27 MW, voltage deviation is 0.1644 p.u and L-index is 0.1152 while the multi-objective functions all together minimized active power and voltage deviation are 4.61 (MW) and 0.1679 p.u. After that CDTBO method has been tested the obtained optimal cost is 14552.55 $/h, emission 0.2053 (t/h), carbon tax is 4.11 ($/h), transmission losses is 3.16 MW, voltage deviation is 0.1542 p.u and L-index is 0.1149 whereas for multi-objective function simultaneously minimized active power and voltage deviation are 4.73 (MW) and 0.1665 p.u. The results has been displayed in Tables 5 and 6 which warranted the usefulness of CDTBO more than DTBO to attain the optimal result in every respect. Seven cases of the OPF-CHPED setup are appraised with DTBO & CDTBO, & assessment were performed to estimate the dominance of the CDTBO technique over DTBO. The diverse comparison of CHPED-OPF setup for cost, emission, power losses, voltage deviation are displayed in Fig. 5. The convergence plot of the considered CDTBO & DTBO optimization method are presented in Fig. 7. The optimal solution by CDTBO of several objectives has been arrived within smaller iterations as opposed to DTBO. The present study ascertained the rapidness of computational duration of CDTBO for combining the chaotic based learning with DTBO tool. The judgment of statistical scrutiny subsequent to 100 iterations with minimum amount, maximum amount and average amount of utilized DTBO & CDTBO are provided in Table 7. The disparity of maximum value, minimum value & average value is very little while CDTBO is used in contrast to DTBO. It provides the evidence of robustness of recommended CDTBO.

5.0.2. Test system-2

Furthermore, to obtain the efficient resolution over cost minimization & emission reduction with optimal flow of power in transmission line, renewable energies are included with planned CHPED based OPF structure. The arrangement turn into more composite due to existence of uncertainties of wind pace. Total 25 wind turbine has been used in integrated wind generating unit. Different wind parameters is displayed in Appendix Table A.3. In CHPED system two-power only units, four-cogeneration units & a heat only unit are connected. On this suggested renewable based CHPED structure, a power only unit is substituted by wind unit. In IEEE-30 bus system, the wind generator is connected to bus-2. The entire load demand is 283.4 MW while reactive power & heat demand are 126.2 MVar & 175 MWth. An outline of IEEE 30 bus setup for OPF-CHPED (with wind power) is given at Table 8. The simulation outcomes of DTBO & CDTBO and finest setting of control variables are displayed on Tables 9 and 10. This suggested renewable-based CHPED-OPF system has been subjected to an analogous analysis using the DTBO and CDTBO to evaluate the quality of the recommended optimization tool for single & multi objective functions. With DTBO the derived optimal cost is 14488.83 $/h, emission 0.1894 (t/h), carbon tax is 3.788 ($/h), transmission losses is 3.19 MW, voltage

Table A.1
Cost and emission coefficients of thermal units for IEEE 30-bus network.

Generator	Bus	a	b	c	d	e	α	β	γ	ω	μ
TG1 (POU)	1	0	2	0.00375	18	0.037	4.091	−5.554	6.49	0.0002	2.857
TG2 (POU)	2	0	1.75	0.0175	16	0.038	2.543	−6.047	5.638	0.0005	3.333
TG5 (CHP)	5	0	1	0.0625	14	0.04	4.258	−5.094	4.586	0.000001	8
TG8 (CHP)	8	0	3.25	0.00834	12	0.045	5.326	−3.55	3.38	0.002	2
TG11 (CHP)	11	0	3	0.025	13	0.042	4.258	−5.094	4.586	0.000001	8
TG13 (CHP)	13	0	3	0.00834	13.5	0.041	6.131	−5.555	5.151	0.00001	6.667

Table A.2
Generation limits and cost co-efficient of HOU.

UNIT	Bus	Hmin (MWTh)	Hmax (MWTh)	α	β	γ
HOU	31	0	2695.2	0.038	2.0109	950

deviation is 0.1494 p.u and L-index is 0.1153 whereas for multi-objective function simultaneously minimized active power and voltage deviation are 4.2 (MW) and 0.1682 p.u. After the CDTBO scheme has been experimented the acquired optimal cost is 14459.26 $/h, emission 0.1886 (t/h), carbon tax is 3.77 ($/h), transmission losses is 3.08 MW, voltage deviation is 0.1487 p.u & decreased L-index is 0.1144 while for multi-objective function concurrently minimized active power and voltage deviation are 4.32 (MW) and 0.1642 p.u. The statistical scrutiny has been conducted over DTBO & CDTBO for OPF-CHPED system (with renewable power) & provided in Table 11 which establishes the robustness of the CDTBO procedure. The different assessment of CHPED-OPF system for cost, emission, power losses, voltage deviation are displayed in Fig. 6. The convergence natures of diverse objective functions are exposed in Fig. 7, where the obtained results in all the cases using CDTBO converges smoothly to the optimum value which is much earlier than the DTBO optimization technique. In addition, it is detected that once incorporating renewable power sources with CHPED-OPF system optimal answer has obtained on single and multi-objective functions are displayed in Tables 12 and 13. Authors have solved the CHPED problem using AFDB-ARO [40], dFDB-SFS [42], FDB-AGSK [43], FDB-TLABC [44], FDB-AEO [45], FDB-LFD [46], FDB-AGDE [47], LRFDB-COA [48], FDB-SFS [49] and FDB-CHOA [50] and a comparison has been made with the proposed CDTBO and DTBO which has been displayed in Table 14. Proposed method has also been compared using the Friedman test method, illustrated in Table 15. Comparative study judge the superiority of the CDTBO technique. Hence it also proved that proposed CDTBO has better dealing capability with non-linear functions.

6. Conclusions and future scopes

The prime objective of this presentation is to demonstrate the scheduling of CHPED based OPF with non-conventional energy sources and depicted the effectiveness of the CDTBO optimization technique. The following list includes the proposed work's most successful contributions:

- A new integrated CHPED based OPF system has been illustrated where 7 units CHPED system is integrated with IEEE-30 bus system for optimal power flow in the transmission line with economic operation.
- Further a renewable energy is integrated with CHPED based OPF system to reduce the utility of thermal units for economic power generation and diminished the emission to save the environment from greenhouse effect.
- The adopted model provides the optimal solution over different objective functions with economic operation of cost, emission minimization, transmission losses minimization, carbon tax minimization, voltage deviation minimization and minimizing the voltage stability indicator L-index. These are the evidence of more efficacy, effectiveness and reliability from the traditional scheduling model.
- In order to balance the exploration and exploitation phases, the various control parameters of the DTBO and CDTBO have been effectively used, which has concluded in the determination of a completely adequate global solution.
- The outcomes of various case studies demonstrate that the suggested CDTBO can reduced generating costs, emissions, transmission losses, voltage deviation, and L-index of the conventional scheduling model.
- In comparison to the DTBO method, CDTBO appears to produce better results.

Future Scopes:

- In future, FACTS devices may be incorporated in the CHPED based OPF problem to improve voltage stability and voltage deviation of power system.
- Utilization of renewable energy sources is a crucial concern with improvising fossil fuel.
- In future, hydro-thermal scheduling may be implemented in CHPED base OPF with different types of renewable sources for economic power generation of power system under pollution free environment.

Funding

This research received no specific grant from any funding agency in the public, commercial, or not-for-profit sectors.

Code availability

The data that support the findings of this study are available from the corresponding author upon reasonable request.

Ethics approval

All authors have been personally and actively involved in substantial work leading to the paper, and will take public responsibility for its content.

Consent for publication

We, the authors, give consent for the publication of identifiable details, which can include photograph(s) and/or videos and/or case history and/or details within the text to be published in the above Article.

CRediT authorship contribution statement

Chandan Paul: Writing – original draft. **Tushnik Sarkar:** Writing – original draft. **Susanta Dutta:** Software. **Provas Kumar Roy:** Software, Writing – review & editing.

Declaration of competing interest

The authors do hereby declare that there is no conflict of interest between the study and others.

Table A.3
Wind parameters.

Specifications wind power unit					
Wind farm	No. of. turbines	Rated power Pwr (MW)	Weibull PDF parameters	Cost coefficient ($/MWh)	
				Reserve, KRw	Penalty, KPw
WG5(bus 2)	25	75	$\xi = 9,\ \kappa = 2$	3	1.5

Data availability

Data will be made available on request.

Appendix

See Tables A.1–A.3.

References

[1] M. Thomson, P. Twigg, B. Majeed, N. Ruck, Statistical process control based fault detection of CHP units, Control Eng. Pract. 8 (1) (2000) 13–20.

[2] A. Sashirekha, J. Pasupuleti, N. Moin, C.S. Tan, Combined heat and power (CHP) economic dispatch solved using Lagrangian relaxation with surrogate subgradient multiplier updates, Int. J. Electr. Power Energy Syst. 44 (1) (2013) 421–430.

[3] P. Fortenbacher, T. Demiray, Linear/quadratic programming-based optimal power flow using linear power flow and absolute loss approximations, Int. J. Electr. Power Energy Syst. 107 (2019) 680–689.

[4] M. Pourakbari-Kasmaei, J.R.S. Mantovani, Logically constrained optimal power flow: Solver-based mixed-integer nonlinear programming model, Int. J. Electr. Power Energy Syst. 97 (2018) 240–249.

[5] T. Leveringhaus, L. Kluß, I. Bekker, L. Hofmann, Solving combined optimal transmission switching and optimal power flow sequentially as convexificated quadratically constrained quadratic program, Electr. Power Syst. Res. 212 (2022) 108534.

[6] J.A. Delgado, E.C. Baptista, A.R. Balbo, E.M. Soler, D.N. Silva, A.C. Martins, L. Nepomuceno, A primal–dual penalty-interior-point method for solving the reactive optimal power flow problem with discrete control variables, Int. J. Electr. Power Energy Syst. 138 (2022) 107917.

[7] S.D. Beigvand, H. Abdi, M. La Scala, Combined heat and power economic dispatch problem using gravitational search algorithm, Electr. Power Syst. Res. 133 (2016) 160–172.

[8] A. Meng, P. Mei, H. Yin, X. Peng, Z. Guo, Crisscross optimization algorithm for solving combined heat and power economic dispatch problem, Energy Convers. Manage. 105 (2015) 1303–1317.

[9] N. Ghorbani, Combined heat and power economic dispatch using exchange market algorithm, Int. J. Electr. Power Energy Syst. 82 (2016) 58–66.

[10] E. Davoodi, K. Zare, E. Babaei, A GSO-based algorithm for combined heat and power dispatch problem with modified scrounger and ranger operators, Appl. Therm. Eng. 120 (2017) 36–48.

[11] C. Paul, P.K. Roy, V. Mukherjee, Optimal solution of combined heat and power dispatch problem using whale optimization algorithm, Int. J. Appl. Metaheuristic Comput. (IJAMC) 13 (1) (2022) 1–26.

[12] M. Ramachandran, S. Mirjalili, M. Nazari-Heris, D.S. Parvathysankar, A. Sundaram, C.A.R.C. Gnanakkan, A hybrid grasshopper optimization algorithm and harris hawks optimizer for combined heat and power economic dispatch problem, Eng. Appl. Artif. Intell. 111 (2022) 104753.

[13] M.A. Al-Betar, M.A. Awadallah, S.N. Makhadmeh, I.A. Doush, R.A. Zitar, S. Alshathri, M. Abd Elaziz, A hybrid Harris Hawks optimizer for economic load dispatch problems, Alex. Eng. J. 64 (2023) 365–389.

[14] M. Gholamghasemi, E. Akbari, M.B. Asadpoor, M. Ghasemi, A new solution to the non-convex economic load dispatch problems using phasor particle swarm optimization, Appl. Soft Comput. 79 (2019) 111–124.

[15] K. Bhattacharjee, A. Bhattacharya, S.H. nee Dey, Solution of economic emission load dispatch problems of power systems by real coded chemical reaction algorithm, Int. J. Electr. Power Energy Syst. 59 (2014) 176–187.

[16] X. Yuan, P. Wang, Y. Yuan, Y. Huang, X. Zhang, A new quantum inspired chaotic artificial bee colony algorithm for optimal power flow problem, Energy Convers. Manage. 100 (2015) 1–9.

[17] S. Dutta, P.K. Roy, D. Nandi, Optimal location of UPFC controller in transmission network using hybrid chemical reaction optimization algorithm, Int. J. Electr. Power Energy Syst. 64 (2015) 194–211.

[18] P.K. Roy, C. Paul, Optimal power flow using krill herd algorithm, Int. Trans. Electr. Energy Syst. 25 (8) (2015) 1397–1419.

[19] J.-O. Lee, Y.-S. Kim, J.-H. Jeon, Optimal power flow for bipolar DC microgrids, Int. J. Electr. Power Energy Syst. 142 (2022) 108375.

[20] A.M. Shaheen, A.M. Elsayed, A.R. Ginidi, R.A. El-Sehiemy, E. Elattar, A heap-based algorithm with deeper exploitative feature for optimal allocations of distributed generations with feeder reconfiguration in power distribution networks, Knowl.-Based Syst. 241 (2022) 108269.

[21] S. Ramesh, E. Verdú, K. Karunanithi, S. Raja, et al., An optimal power flow solution to deregulated electricity power market using meta-heuristic algorithms considering load congestion environment, Electr. Power Syst. Res. 214 (2023) 108867.

[22] A.A. El-Fergany, H.M. Hasanien, Tree-seed algorithm for solving optimal power flow problem in large-scale power systems incorporating validations and comparisons, Appl. Soft Comput. 64 (2018) 307–316.

[23] H. Xiao, Z. Dong, L. Kong, W. Pei, Z. Zhao, Optimal power flow using a novel metamodel based global optimization method, Energy Procedia 145 (2018) 301–306.

[24] K. Abaci, V. Yamacli, Differential search algorithm for solving multi-objective optimal power flow problem, Int. J. Electr. Power Energy Syst. 79 (2016) 1–10.

[25] H.R. Bouchekara, A. Chaib, M.A. Abido, R.A. El-Sehiemy, Optimal power flow using an Improved Colliding Bodies Optimization algorithm, Appl. Soft Comput. 42 (2016) 119–131.

[26] A.R. Bhowmik, A.K. Chakraborty, Solution of optimal power flow using non dominated sorting multi objective opposition based gravitational search algorithm, Int. J. Electr. Power Energy Syst. 64 (2015) 1237–1250.

[27] A. Mukherjee, P.K. Roy, V. Mukherjee, Transient stability constrained optimal power flow using oppositional krill herd algorithm, Int. J. Electr. Power Energy Syst. 83 (2016) 283–297.

[28] B. Mandal, P.K. Roy, Multi-objective optimal power flow using quasi-oppositional teaching learning based optimization, Appl. Soft Comput. 21 (2014) 590–606.

[29] S. Hazra, P.K. Roy, Solar-wind-hydro-thermal scheduling using moth flame optimization, Optim. Control Appl. Methods (2021).

[30] C. Paul, P.K. Roy, V. Mukherjee, Chaotic whale optimization algorithm for optimal solution of combined heat and power economic dispatch problem incorporating wind, Renew. Energy Focus 35 (2020) 56–71.

[31] C. Paul, P. Kumar Roy, V. Mukherjee, Study of wind-solar based combined heat and power economic dispatch problem using quasi-oppositional-based whale optimization technique, Optim. Control Appl. Methods (2021).

[32] C. Paul, P.K. Roy, V. Mukherjee, Application of chaotic quasi-oppositional whale optimization algorithm on CHPED problem integrated with wind-solar-EVs, Int. Trans. Electr. Energy Syst. 31 (11) (2021) e13124.

[33] Z. Zhang, L. Shang, C. Liu, Q. Lai, Y. Jiang, Consensus-based distributed optimal power flow using gradient tracking technique for short-term power fluctuations, Energy 264 (2023) 125635.

[34] S.I. Evangeline, P. Rathika, Wind farm incorporated optimal power flow solutions through multi-objective horse herd optimization with a novel constraint handling technique, Expert Syst. Appl. 194 (2022) 116544.

[35] S. Li, W. Gong, L. Wang, Q. Gu, Multi-objective optimal power flow with stochastic wind and solar power, Appl. Soft Comput. 114 (2022) 108045.

[36] T. Chen, A.Y. Lam, Y. Song, D.J. Hill, Fast tuning of transmission power flow routers for transient stability constrained optimal power flow under renewable uncertainties, Electr. Power Syst. Res. 213 (2022) 108735.

[37] M.H. Sulaiman, Z. Mustaffa, M.I.M. Rashid, An application of teaching–learning-based optimization for solving the optimal power flow problem with stochastic wind and solar power generators, Res. Control Optim. 10 (2023) 100187.

[38] P.P. Biswas, P. Suganthan, G.A. Amaratunga, Optimal power flow solutions incorporating stochastic wind and solar power, Energy Convers. Manage. 148 (2017) 1194–1207.

[39] M. Basu, Dynamic optimal power flow for isolated microgrid incorporating renewable energy sources, Energy 264 (2023) 126065.

[40] B. Ozkaya, S. Duman, H.T. Kahraman, U. Guvenc, Optimal solution of the combined heat and power economic dispatch problem by adaptive fitness-distance balance based artificial rabbits optimization algorithm, Expert Syst. Appl. 238 (2024) 122272.

[41] B. Ozkaya, H.T. Kahraman, S. Duman, U. Guvenc, M. Akbel, Combined heat and power economic emission dispatch using dynamic switched crowding based multi-objective symbiotic organism search algorithm, Appl. Soft Comput. 151 (2024) 111106.

[42] H.T. Kahraman, M.H. Hassan, M. Katı, M. Tostado-Véliz, S. Duman, S. Kamel, Dynamic-fitness-distance-balance stochastic fractal search (dFDB-SFS algorithm): an effective metaheuristic for global optimization and accurate photovoltaic modeling, Soft Comput. (2023) 1–28.

[43] H. Bakır, S. Duman, U. Guvenc, H.T. Kahraman, Improved adaptive gaining-sharing knowledge algorithm with FDB-based guiding mechanism for optimization of optimal reactive power flow problem, Electr. Eng. (2023) 1–40.
[44] S. Duman, H.T. Kahraman, Y. Sonmez, U. Guvenc, M. Kati, S. Aras, A powerful meta-heuristic search algorithm for solving global optimization and real-world solar photovoltaic parameter estimation problems, Eng. Appl. Artif. Intell. 111 (2022) 104763.
[45] Y. Sonmez, S. Duman, H.T. Kahraman, M. Kati, S. Aras, U. Guvenc, Fitness-distance balance based artificial ecosystem optimisation to solve transient stability constrained optimal power flow problem, J. Exp. Theor. Artif. Intell. (2022) 1–40.
[46] H. Bakir, U. Guvenc, H.T. Kahraman, S. Duman, Improved Lévy flight distribution algorithm with FDB-based guiding mechanism for AVR system optimal design, Comput. Ind. Eng. 168 (2022) 108032.
[47] U. Guvenc, S. Duman, H.T. Kahraman, S. Aras, M. Katı, Fitness–Distance Balance based adaptive guided differential evolution algorithm for security-constrained optimal power flow problem incorporating renewable energy sources, Appl. Soft Comput. 108 (2021) 107421.
[48] S. Duman, H.T. Kahraman, U. Guvenc, S. Aras, Development of a Lévy flight and FDB-based coyote optimization algorithm for global optimization and real-world ACOPF problems, Soft Comput. 25 (2021) 6577–6617.
[49] S. Aras, E. Gedikli, H.T. Kahraman, A novel stochastic fractal search algorithm with fitness-distance balance for global numerical optimization, Swarm Evol. Comput. 61 (2021) 100821.
[50] H. Bakir, H.T. Kahraman, S. Temel, S. Duman, U. Guvenc, Y. Sonmez, Development of an FDB-based chimp optimization algorithm for global optimization and determination of the power system stabilizer parameters, in: The International Conference on Artificial Intelligence and Applied Mathematics in Engineering, Springer, 2021, pp. 337–365.
[51] M. Dehghani, E. Trojovská, P. Trojovskỳ, A new human-based metaheuristic algorithm for solving optimization problems on the base of simulation of driving training process, Sci. Rep. 12 (1) (2022) 9924.
[52] A. Pai, Energy Function Analysis for Power System Stability, Springer Science & Business Media, 1989.